Bioorganic Chemistry 107 (2021) 104525

Contents lists available at ScienceDirect

Bioorganic Chemistry

journal homepage: www.elsevier.com/locate/bioorg

Probing phenylcarbamoylazinane-1,2,4-triazole amides derivatives as lipoxygenase inhibitors along with cytotoxic, ADME and molecular docking studies

Saima Muzaffar [a], Wardah Shahid [a], Naheed Riaz [a,*], Muhammad Saleem [a], Muhammad Ashraf [a,*], Aziz-ur-Rehman [b], Bushra Bashir [a], Ayesha Kaleem [a], Mariya al-Rashida [c], Bikash Baral [d], Keshab Bhattarai [e], Harald Gross [e]

[a] Department of Chemistry, Baghdad-ul-Jadeed Campus, The Islamia University of Bahawalpur, Bahawalpur 63100, Pakistan
[b] Department of Chemistry, Government College University Lahore, Lahore 54000, Pakistan
[c] Department of Chemistry, Forman Christian College (A Chartered University), Ferozepur Road Lahore, Lahore 54600, Pakistan
[d] Department of Biochemistry, University of Turku, Tykistökatu 6, Finland
[e] Department of Pharmaceutical Biology, Auf der Morgenstelle 8, 72076, University of Tuebingen, Tuebingen, Germany

ARTICLE INFO

Keywords:
Lipoxygenase inhibition
Cytotoxicity
ADME & Molecular docking studies
Azinanetriazoles
Synthesis

ABSTRACT

Hunting small molecules as anti-inflammatory agents/drugs is an expanding and successful approach to treat several inflammatory diseases such as cancer, asthma, arthritis, and psoriasis. Besides other methods, inflammatory diseases can be treated by lipoxygenase inhibitors, which have a profound influence on the development and progression of inflammation. In the present study, a series of new *N*-alkyl/aralky/aryl derivatives (**7a-o**) of 2-(4-phenyl-5-(1-phenylcarbamoyl)piperidine-4*H*-1,2,4-triazol-3-ylthio)acetamide was synthesized and screened for their inhibitory potential against the enzyme 15-lipoxygenase. The simple precursor ethyl piperidine-4-carboxylate (**a**) was successively converted into phenylcarbamoyl derivative (**1**), hydrazide (**2**), semicarbazide (**3**) and *N*-phenylated 5-(1-phenylcarbamoyl)piperidine-1,2,4-triazole (**4**), then in combination with electrophiles (**6a-o**) through further multistep synthesis, final products (**7a-o**) were generated. All the synthesized compounds were characterized by FTIR, ^{1}H, ^{13}C NMR spectroscopy, EIMS, and HREIMS spectrometry. Almost all the synthesized compounds showed excellent inhibitory potential against the tested enzyme. Compounds **7c, 7f, 7d,** and **7g** displayed potent inhibitory potential (IC_{50} 9.25 ± 0.26 to 21.82 ± 0.35 μM), followed by the compounds **7n, 7h, 7e, 7a, 7b, 7l,** and **7o** with IC_{50} values in the range of 24.56 ± 0.45 to 46.91 ± 0.57 μM. Compounds **7c, 7f, 7d** exhibited 71.5 to 83.5% cellular viability by MTT assay compared with standard curcumin (76.9%) when assayed at 0.125 mM concentration. *In silico* ADME studies supported the drug-likeness of most of the molecules. *In vitro* inhibition studies were substantiated by molecular docking wherein the phenyl group attached to the triazole ring was making a π-δ interaction with Leu607. This work reveals the possibility of a synthetic approach of compounds in relation to lipoxygenase inhibition as potential lead compounds in drug discovery.

1. Introduction

Inflammation is a complex biological defense mechanism elicited in response to allergens, pathogens and chemicals. When tissue cells are damaged by these effectors, the cell membranes which is enriched in phospholipids are hydrolysed by activated phospholipase A_2 to yield arachidonic acid which in turn enters two separate oxidative pathways called cyclooxygenase (COX) pathway and lipoxygenase (LOX) pathway. Both these pathways result in the formation of functionally active metabolites which act in autocrine, paracrine and endocrine manner [1]. COX-I (EC 1.14.99.1) is constitutive enzyme and is involved in renal homeostasis and platelet aggregation. COX-II (EC 1.14.99.2) is inducible enzyme that converts arachidonic acid into prostaglandin G_2 (PGG_2) which further yields thromboxanes, prostacyclin, prostaglandin E_2 and their increased levels mediate the pain, heat, redness, swelling and the fever [2]. On the other hand, LOX-pathway is characterized by a

* Corresponding authors.
E-mail addresses: nrch322@yaoo.com (N. Riaz), dr.m.ashraf@gmail.com (M. Ashraf).

https://doi.org/10.1016/j.bioorg.2020.104525
Received 2 September 2020; Received in revised form 24 October 2020; Accepted 30 November 2020
Available online 3 December 2020

family of enzymes involved to convert arachidonic acid into a variety of hydroperoxy acids and ultimately end up in another class of functionally active molecules called leukotrienes (LT) like LTA_4, LTB_4, LTC_4, LTD_4, LTE_4 etc. and these leukotrienes are mediators of allergic response and inflammation [3]. The symptoms include fatigue, sinusitis, cataracts, pain, heart disease, stroke, asthma, arthritis, colitis etc. Therefore, the inhibition of COX and LOX pathways by drugs can give some relief to patients with asthma, pain, allergy and other inflammatory diseases like cancer. In LOX pathway, lipoxygenases (LOXs, EC 1.13.11.12) are family of enzymes present across multiple species from plants to mammals [3]. In humans, six family members have been sequenced and characterized. Seven members have been described in mice. Classification is based on the product produced due to the specificity of the substrate, linoleic acid or arachidonic acid. Stereospecific incorporation of molecular oxygen occurs at carbons 5, 8, 9, 11, 12, and 15 leading to the corresponding regioisomeric hydroperoxyeicosatetraenoic acids (HPETEs) [4]. This diversity in the function across this family of enzymes has resulted in confounding results, which are recently beginning to be clarified. All these enzymes trigger the synthesis of important biological secondary metabolites and have been involved in inflammation [3]. For example, 12-LOX is involved in the pathogenesis and complications of diabetes mellitus [5]. 15-LOX is involved in the promotion of cancer by amplifying peroxisome proliferator-activated receptor-gamma (PPARγ) [6]. Recently, it has been reviewed that 15-LOX inhibitors might be suitable as chemotherapy agents in the near future especially for the prostrate cancer [7]. The metal cofactor of these enzymes alters its oxidation state Fe^{+2}, Fe^{+3} in their catalytic redox reaction, while inserting oxygen into the polyunsaturated fatty acid substrate (arachidonic acid or linoleic acid), synthesizing a large variety of biologically active intermediates called leukotrienes. Leukotrienes are inflammatory mediators playing a pathophysiological role in different diseases like asthma, allergic rhinitis, cardiovascular diseases, Alzheimer's disease, osteoporosis, atherosclerosis, Crohn's disease, multiple sclerosis, osteoarthritis, psoriasis, rheumatoid arthritis, diabetes mellitus, carcinoma, bacterial or viral infections which leads to severe inflammation and certain types of cancers [8]. Therefore, the regulation of polyunsaturated fatty acid metabolizing enzymes is a great challenge and many inflammatory and allergic disorders could be cured by inhibition of family of LOX enzymes. However, the development of specific inhibitors has been hampered by homology of LOX family members. Todate no pharmaceutical product from 15-LOX inhibitors has been approved for therapeutic usage except Zileuton (N-[1-(1-benzothien-2-yl)ethyl]-*N*-hydroxyurea) that is marketed for the treatment of asthma [9]. Its side effects include sinusitis, nausea and pharyngolaryngeal pain. Thus, the search for LOX inhibitors with minimal side effects is crucial. Among others, the triazoles were identified as good inhibitors of human 15-LOX and 5-LOX [10].

1,2,4-Triazoles, a group of heterocyclic compounds, and their fused heterocyclic derivatives have acquired much attention in the last few decades due to their diverse chemistry [11]. They interact at the active site of a receptor as hydrogen bond acceptor and as a donor, triazole core acts as an important pharmacophore [12]. Moreover, good stability to acid-base hydrolysis and oxidative-reductive conditions and resistance to metabolic degradation are such desirable properties that make it a medicinal backbone and important area of research in a wide range of applications in organic and bioorganic synthesis [13], like plant growth regulators, drug designing, surfactants, agrochemicals and complexation agents [11]. Literature quest revealed that 1,2,4-triazoles derivatives possess significant antibacterial, antiviral, antifungal, antituberculosis, antidepressant, antiinflammatory, anticancer, antioxidant, antitumor, anticonvulsant [14], molluscicidal, analgesic, antihypertensive, anti-HIV-1, diuretic, anthelmintic, bactericidal, herbicidal, insecticidal, acaricidal, fungicidal, antileishmanial, anxiolytic, hypolipidemic, antimycotic, antimigraine, antinociceptive, CNS stimulants, antianxiety and antiplatelet activities [15]. Furthermore, 1,2,4-triazole derivatives have been reported to exhibit good inhibitory potential against many enzymes like aromatase, cholinesterase, tumor-associated carbonic anhydrase [16], xanthine oxidoreductase [17], methionine aminopeptidase-2 [18], lipase, β-hydroxysteroid dehydrogenase type-1, CYP26A1, adenosine deaminase, thymidine phosphorylase [19], and LOX [20].

The purpose of the present research work was to explore a new series of biologically active mercapto *N*-alkyl/aralkyl/aryl acetamide triazoles which may assist in designing new synthetic drug leads. In the present studies, *N*-substituted derivatives (**7a-o**) of 1,2,4-triazol-3-ylthio)acetamide were synthesized in a series of steps and were subsequently screened against 15-LOX.

2. Results and discussion

2.1. Chemistry

The present study aimed to synthesize new phenyl carbamoyl piperidine-1,2,4-triazole amides (**7a-o**) (Fig. 1) containing a variety of substituents and to investigate them for their enzyme inhibitory potential against enzyme 15-LOX. All the synthetic protocols are outlined in Scheme 1. The simplest starting material isonepacotate (**a**), was rubbed with phenylisocyanate and then treated with hydrazine hydrate to get hydrazide **2** (98% yield). The ^{1}H NMR spectrum of **2** showed two singlets at δ 4.02 (1H, –NH) and 8.90 (2H, $–NH_2$) attributed to $–NHNH_2$ moiety. The reaction of the hydrazide (**2**) with phenyl isothiocyanate yielded *N*-phenyl-4-(2-(phenylcarbamothioyl)hydrazinecarbonyl)piperidine-1-carboxamide (**3**) which was refluxed under alkaline conditions (10% NaOH), to get an intramolecular cyclized product, 4-(5-mercapto-4-phenyl-4H-1,2,4-triazol-3-yl)-*N*-phenylpiperdine-1-carboxamide (**4**). These intermediates were identified through ^{1}H NMR analysis, since *N*-phenyl nuclei in the spectrum of **3** resonated at δ 7.25 (5H, br s, *N*-Ph) in addition to signals of phenyl carbamoyl moiety at δ 7.19 (1H, t, J = 7.5 Hz, H-4′), 7.43 (2H, t, J = 7.5 Hz, H-3′,5′), 7.61 (2H, d, J = 7.5 Hz, H-2′,6′). Further, the C═S carbon nucleus resonated at δ 181.1 in the ^{13}C NMR spectrum of **3**, whereas, the -SH proton displayed its position at δ 11.2 in the ^{1}H NMR spectrum of compound **4**. The absence of –NH signal and carbonyl carbon resonance in their respective NMR spectra substantiated the successful conversion of **3** into phenyl substituted 1,2,4-triazol-3-thiol (**4**). The *N*-alkyl/aralky/aryl-2-bromoacetamides (**6a-o**), the second precursors of target compounds were synthesized by stirring alkyl/aralkyl/aryl amines (**5a-o**) (Table 1) with 2-bromoacetyl bromide in a basic medium (pH 9–10). The final step was the coupling of compound **4** separately with the precursors **6a-o** to get target compounds **7a-o**, respectively. This task was accomplished according to the procedures given in the experimental section.

The compound **7a** was synthesized as a colorless amorphous powder (93% yield; M.P. 98-100℃). Its IR spectrum displayed the absorption bands at 3365, 3045, 2941, 1681, 1662, 1619–1544, 1260 cm^{-1} represented the presence of N—H, Ar-H, C—H, C═O, C═C, C═N, C—N functional groups, respectively. The ^{1}H NMR spectrum exhibited two sets of *N*-ethyl groups at δ 1.10 (3H, t, J = 7.1 Hz, H-2‴), 1.22 (3H, t, J = 7.1 Hz, H-2⁗), and 3.35 (2H, q, J = 7.1 Hz, H-1‴), 3.45 (2H, q, J = 7.1 Hz, H-1⁗), respectively. The signals at δ 1.81 (4H, m, H-3′,5′), 1.86 (1H, m, H-4′) and 2.84 (4H, m, H-2′,6′) supported the existence of azinane ring coupled to 1,2,4 triazole. Methylene of acetamide was determined by singlet appeared at δ 4.14 (2H, s, H-2‴). The signal appeared at δ 7.48 (2H, m), 7.64 (3H, m) was assigned to the phenyl group bonded to a nitrogen atom of triazole while the presence of two triplets at δ 7.00 (1H, J = 7.5 Hz, H-4″), 7.24 (2H, J = 7.5 Hz, H-3″,5″) together with a doublet at δ 7.32 (2H, J = 7.5 Hz, H-2″,6″) in aromatic zone confirmed the presence of second phenyl group in the molecule. The BB & DEPT spectra of ^{13}C NMR showed altogether twenty carbon signals for 26 carbons which supported the presence of two methyl, five methylene, seven methine, and six quaternary carbon atoms. The most downfield peaks at δ 166.8, 158.7, 156.4, and 151.4 were allotted to two amide carbonyls and two quaternary carbons of triazole ring, respectively. The signal at δ 35.4 was attested for methylene carbon atom bonded to S-

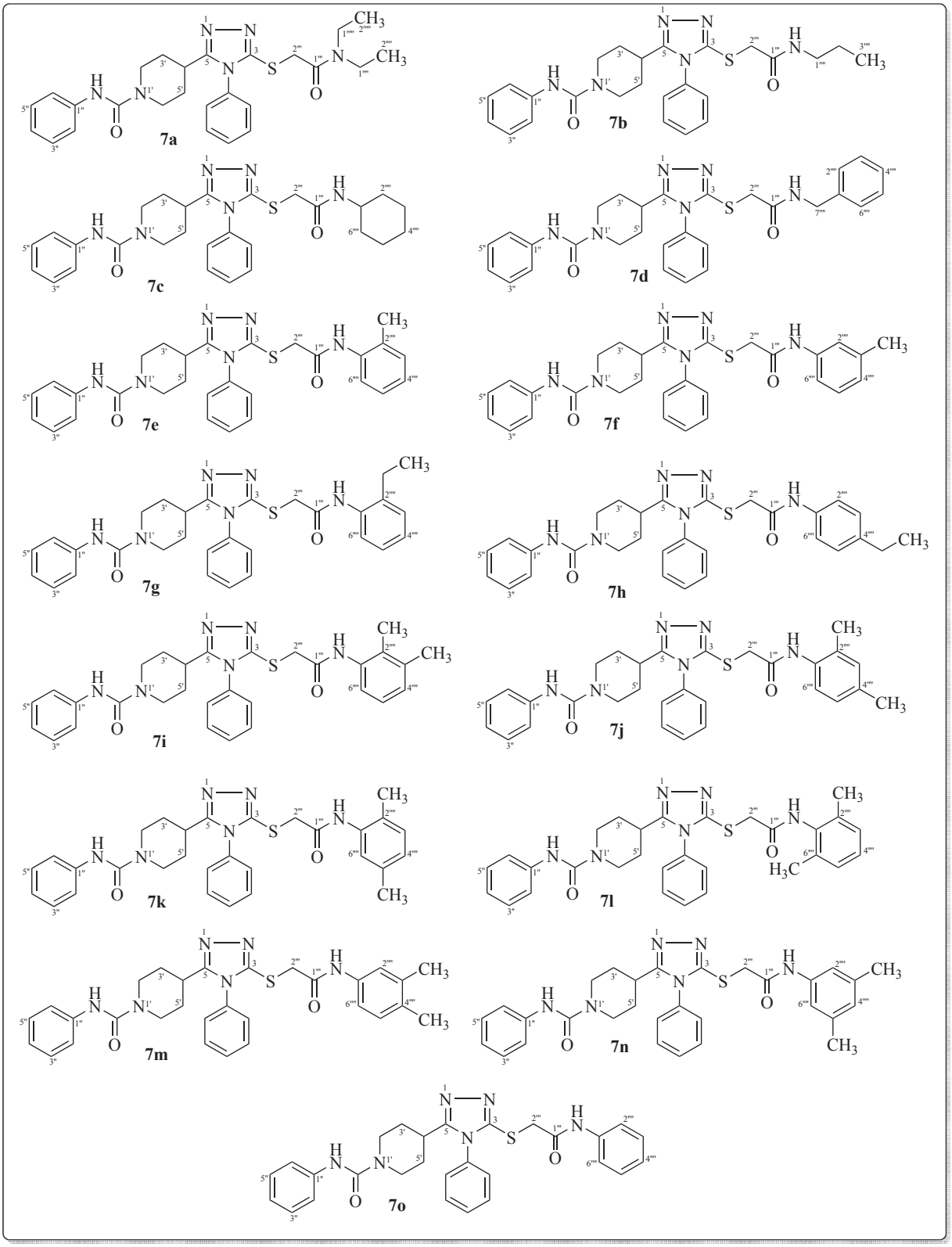

Fig. 1. Chemical scaffolds of the synthesized compounds.

atom. The presence of azinane ring was confirmed due to the carbon signals at δ 43.5, 32.8, and 29.9. The signals for *N*-ethyl groups resonated at δ 42.5, 40.7, 13.0, and 11.7. The C-peaks at δ 139.6, 128.2, 122.7, and 120.8 were assigned to the phenyl ring of phenylcarbamoyl moiety, whereas, the signals at δ 132.8, 130.4, 130.0, 127.5 were attributed to the phenyl moiety attached to triazole nucleus. The molecular formula $C_{26}H_{32}N_6O_2S$ of **7a** was deduced through HR-EI-MS which showed the molecular ion $[M]^+$ peak at *m/z* 442.2330. The structure elucidation of the remaining compounds **7b-o** of the series was done in the similar fashion and their spectral data is presented in the

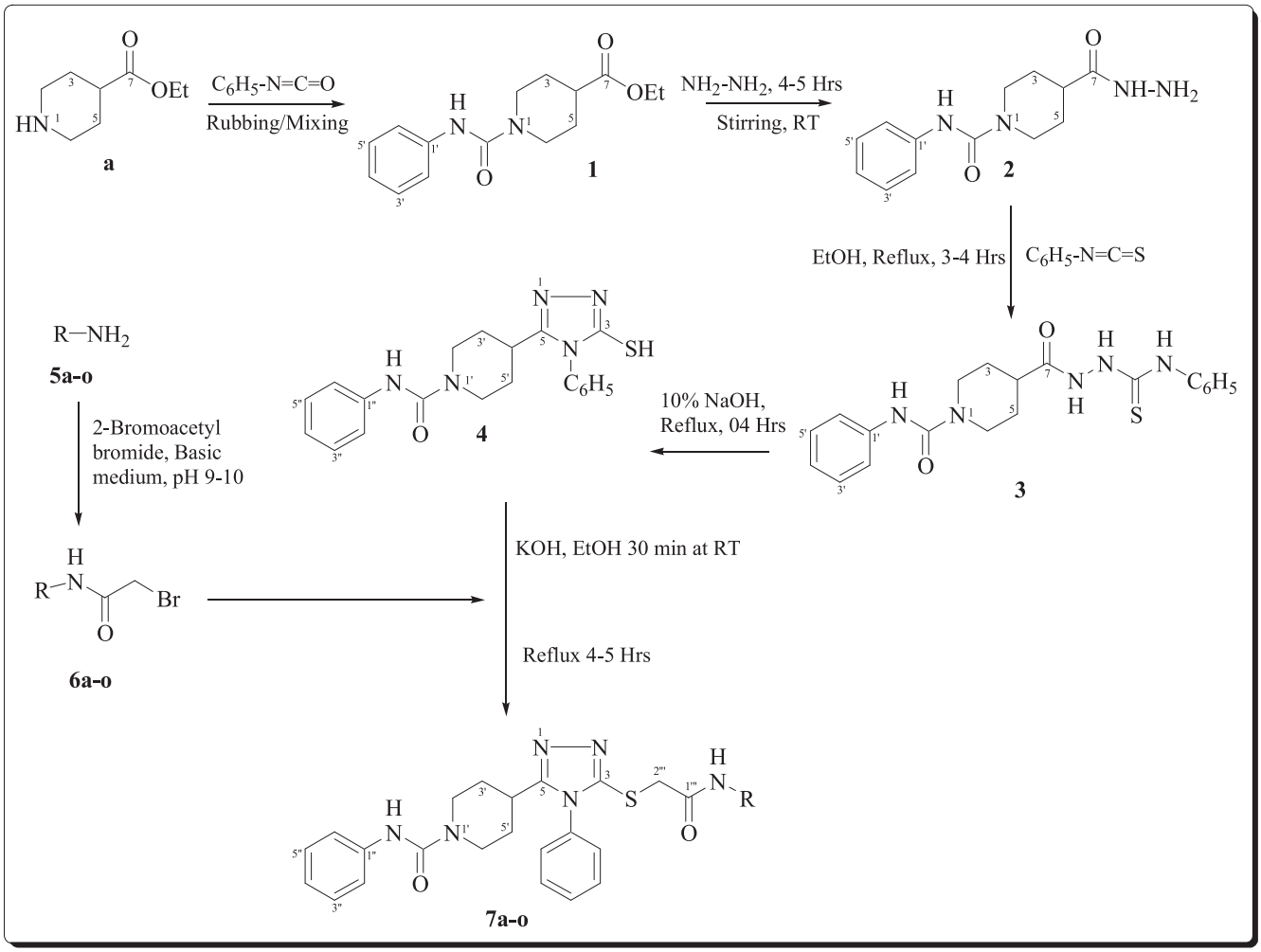

Scheme 1. Protocol for the synthesis of triazole amides (**7a-o**) from isonepacotate.

Table 1
. Alkyl/aralkyl/aryl-substituted amines.

Compd	R	Compd	R	Compd	R
a	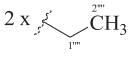	f	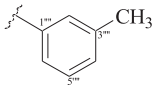	k	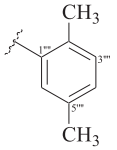
b	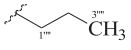	g	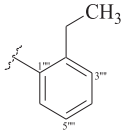	l	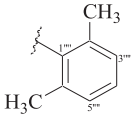
c	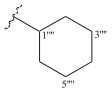	h	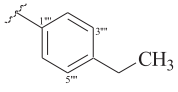	m	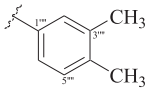
d	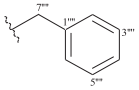	i	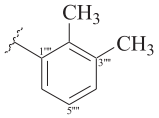	n	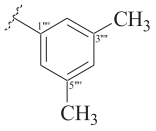
e	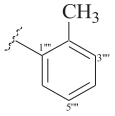	j	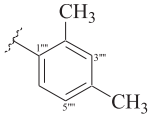	o	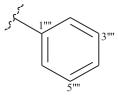

experimental section.

2.2. Lipoxygenase inhibitory activities and SAR studies

In vitro 15-LOX inhibition of compounds **7a-o** was ascertained using quercetin (IC_{50} 4.86 ± 0.14 μM) as standard; the results are given in Table 2. All the compounds exhibited significant inhibitory activity (9.25 ± 0.26 to 56.35 ± 0.84 μM) against the tested enzyme. **7c** and **7f** showed the most potent 15-LOX inhibition with IC_{50} values of 9.25 ± 0.26 and 9.54 ± 0.17 μM, respectively. Even though the activity is cumulative of the entire molecule, so for a minimal SAR was conceded by analyzing the consequence of different alkyl/aralkyl/aryl groups on the inhibitory capacity, the way it was the one-off divergent part and all other parts were same in all molecules. The general structural bits of the studied acetamides are sported in Fig. 2.

Comparison of the activities of **7c** (9.25 ± 0.26 μM) and **7d** (13.64 ± 0.24) evinced that unsaturation resulted in a lesser activity that may be caused by the waning of electronic charge, while the comparison of the activity of **7d** (13.64 ± 0.24 μM) with **7f** (9.54 ± 0.17 μM) revealed that substitution of methyl group at meta-position on phenyl ring caused the higher inhibitory potential that may be attributed to mesomaric effect of the methyl group. It is also noticed that the activity is vaster in the nitrogen atom having benzyl structures bound by a methyl linker instead of the compounds directly attached by the phenyl ring. This philosophises that the unpaired electrons of the *N*-atom bonded to the phenyl ring are involved in resonance and that the nitrogen offers little interaction to the enzyme by decreasing the potential for protonation. This methylene bridge effect is supported by the value of diminished inhibiting activity displayed by **7o** (46.91 ± 0.57 μM). Likewise, **7g** and **7n** exhibited potent inhibitory activities with IC_{50} values as 21.82 ± 0.35 and 24.56 ± 0.45 μM, respectively. When comparing the activities of **7g** (21.82 ± 0.35 μM) and **7h** (32.54 ± 0.63 μM) bearing the same substituent, the ethyl group at *ortho* and *para* positions, respectively, it may be deduced that the electron-donating effect of ethyl group attached to phenyl group is lessened in *para* isomer as compared to *ortho* so as showing somewhat lower inhibitory activity. Meanwhile, comparing the activity of **7g** (21.82 ± 0.35 μM) and **7e** (32.61 ± 0.46 μM); unexpectedly the activity is decreased, though the methyl group is more electron-donating than the ethyl group, and indicates that the decrease in size of the substituent subsides activity.

Equipotent activities were manifested by **7a, 7b, 7l** and **7o,** that are 42.53 ± 0.75, 45.47 ± 0.82, 46.38 ± 0.57 and 46.91 ± 0.57 μM, respectively. These comparatively lower activities of **7a** and **7b** demonstrate that alkyl-substituted compounds have lesser inhibitory potential as compared to the aryl-substituted but conversely, **7l** and **7o** demonstrated the same activities. This may be due to the less electronic charge or resonance in phenyl ring. Inspection of the dimethyl substituted derivatives reveales that their inhibitory potential may be on account of stearic effects. From the discussion of the SAR within the synthesized derivatives, it can be conferred that both the positions and type of substituents at the aryl part are playing vital roles in 15-LOX inhibitory activities.

Table 2
15-LOX inhibitory and cytotoxicity profiles of compounds **7a-o** (Mean ± SEM, n = 3).

Compound	Soybean 15-LOX assay		Cell viability assay
	Inhibition (%) at 0.125 mM	IC_{50} (μM)	Cell viability (%) at 0.125 mM
7a	59.81 ± 1.32	42.53 ± 0.75	63.2 ± 1.7
7b	53.46 ± 1.24	45.47 ± 0.82	62.3 ± 1.6
7c	76.54 ± 1.13	9.25 ± 0.26	83.5 ± 1.3
7d	74.21 ± 1.29	13.64 ± 0.24	78.4 ± 1.2
7e	83.25 ± 1.43	32.61 ± 0.46	49.3 ± 1.4
7f	85.58 ± 1.21	9.54 ± 0.17	71.5 ± 1.3
7g	67.61 ± 1.25	21.82 ± 0.35	45.7 ± 1.5
7h	68.48 ± 1.32	32.54 ± 0.63	52.3 ± 1.7
7i	58.19 ± 1.46	56.35 ± 0.84	57.4 ± 1.5
7j	56.42 ± 1.47	52.62 ± 0.83	65.5 ± 1.7
7k	84.51 ± 1.53	51.72 ± 0.72	38.3 ± 1.3
7l	56.47 ± 1.36	46.38 ± 0.57	32.7 ± 1.5
7m	45.42 ± 1.35	Inactive	28.5 ± 1.3
7n	64.13 ± 1.43	24.56 ± 0.45	45.6 ± 1.2
7o	75.56 ± 1.56	46.91 ± 0.57	58.4 ± 1.5
Quercetin	92.63 ± 1.24	4.86 ± 0.14	–
Cyclophosphamide	–	–	58.5 ± 1.6
Cisplatin	–	–	54.7 ± 1.7
Curcumin	–	–	76.9 ± 1.5

2.3. Cell viability studies

Compounds **7a-o** were screened for their cytotoxicity against mononuclear cells purified from fresh blood and used in MTT assay at 0.125 mM concentration [21] (Table 2). Compound **7c** was found to be the least toxic and showed 83.5 ± 1.3% cell viability followed by **7d** that exhibited 78.4 ± 1.2% viability. The highly toxic compound **7m** showed 28.5 ± 1.3% cell viability and was also inactive against the enzyme 15-LOX. The order of increments in cell toxicity was found as **7c** < **7d** < **7f** < **7j** < **7a** < **7b** < **7o** < **7i**. This data reveals that potent inhibitors show greater cell viability and offer their potential candidature as 'lead' compounds against 15-LOX. Compound **7m** was inactive as a 15-LOX inhibitor and was also highly cytotoxic that killed about 73% cells at 0.125 mM concentration in the assayed conditions, even worse than the standard drugs cyclophosphamide, cisplatin, and curcumin (Table 2).

2.4. ADME studies

The computational methods are routinely used for the prediction of molecular properties of the drug molecues which are necessary for their pharmacokinetics studies. These ADME (absorption, distribution, metabolism, and excretion) properties are predicted by Lipinski's rule of five [22]. MedChem Designer software ver 3.0 has been used for these studies (Table 3). The rule states that poor absorption or permeation of drug occurs when it violates this rule, that is, it has >5 hydrogen bond donors, molecular weight is >500, log P is >5 and the sum of N and O atoms is >10.

The lipophilicity is determined by logP, its value < 5.0 predicts a good partition coefficient. S + logP and MlogP are octanol–water distribution coefficients and based on in silico analysis their values < 5 indicate that these molecules have drug-like properties. Higher logD, logP values, and lower number of hydrogen bonds predict higher bioavailability of drugs. TPSA is the topological polar surface area and should be >140 $Å^2$ which is linked with low blood–brain barrier penetration and poor membrane permeability. Further, the sum of hydrogen bond donor and acceptor (M_NO + HBDH) should be ≤12. The data indicates that all these molecules meet the Lipinski's and Veber's rules of good drug-likeness property [22,23].

2.5. Molecular docking studies with soybean 15-LOX enzyme

Molecular docking studies were carried out both for soybean 15-LOX and human 5-LOX. A logical similarity exists amongst the soybean 15-

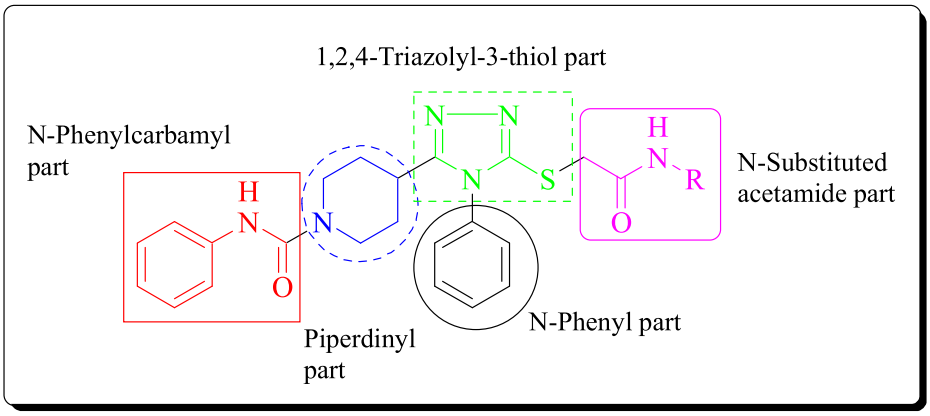

Fig. 2. General structural features of compounds **7a-o**.

Table 3
ADME properties of compounds **7a-o**.

Comp	MlogP	S + logP	S + logD	M. Wt.	M_NO	T_PSA	HBDH
7a	3.614	2.871	2.871	492.647	8	83.36	1
7b	3.410	2.648	2.648	478.620	8	92.15	2
7c	4.209	3.987	3.987	532.712	8	92.15	2
7d	3.995	3.168	3.168	526.664	8	92.15	2
7e	4.263	3.704	3.704	526.664	8	92.15	2
7f	4.263	3.787	3.787	526.664	8	92.15	2
7g	4.456	4.096	4.096	540.691	8	92.15	2
7h	4.456	4.188	4.188	540.691	8	92.15	2
7i	4.456	4.021	4.021	540.691	8	92.15	2
7j	4.456	4.061	4.061	540.691	8	92.15	2
7k	4.456	4.087	4.087	540.691	8	92.15	2
7l	4.456	3.988	3.988	540.691	8	92.15	2
7m	4.456	4.105	4.105	540.691	8	92.15	2
7n	4.456	4.162	4.162	540.691	8	92.15	2
7o	4.068	3.465	3.465	512.637	8	92.15	2

LOX and human 5-LOX that become indistinguishable for more than 50% within 10 Å in the active site pocket [24]. Soybean 15-LOX is the most easily accessible than the human LOX so that its results could be generalized and extendable to human 5-LOX. That is why the docking of compounds has been carried out in the active sites of the enzyme only, 15 Å area around the active site.

The crystal structure of soybean 15-LOX enzyme (PDB id: 1rrh, 2.0 Å) was downloaded from the Protein Data Bank (PDB). All steps of receptor preparation, and subsequesnt docking studies were carried out using BioSolveIT's LeadIT software (LeadIT version 2.3.2; BioSolveIT GmbH, Sankt Augustin, Germany, 2017, www.biosolveit.de/LeadIT). Out of top 10 docked conformations, each conformation was analyzed for its binding free energy using HYDE utility of LeadIT software, the conformation with most favorable binding free energy was selected for detailed binding site interactions (Table 4).

The docked conformation of compound **7c** is shown in Fig. 3. Lys278 was making hydrogen bonds with triazole nitrogen and carbonyl oxygen atom. A π-anion interaction was observed between Asp553 and the phenyl ring connected to piperidinyl amide moiety. A number of hydrophobic interactions were also observed. Tyr275 was making a π-sigma interaction with the cyclohexyl group. An alkyl interaction was observed between Lys278 and the cyclohexyl group. Phe272 and Ala263 were making π-alkyl interactions with piperaine moiety and *N*-substituted phenyl ring. Leu273, Ala777 and Ile857 made π-alkyl interactions with the phenyl ring connected to piperidinyl amide moiety.

The docked conformation of compound **7d** is shown in Fig. 4. Lys278 was making a hydrogen bond with the oxygen atom of the carbonyl group. A π-anion interaction was observed between Asp553 and the phenyl ring connected to piperidinyl amide moiety. A π-sigma interaction was observed between Ala263 and *N*-substituted phenyl ring. A number of π-alkyl interactions were observed. Phe272 was making π-alkyl interaction with the piperidine moiety. Val256 and Leu563 were making π-alkyl interactions with the phenyl ring attached to the amide group. Leu273, Ala777 and Ile857 made π-alkyl interactions with the phenyl ring connected to piperidinyl amide moiety.

The docked conformation of compound **7f** is shown in Fig. 5. Lys278 was making hydrogen bonds with the nitrogen atom of the triazole ring. Phe272 was making a π-sulfur interaction with the sulfur atom. A π-anion interaction was observed between Asp553 and the phenyl ring connected to piperidinyl amide moiety. A π-sigma interaction was observed between Ala263 and *N*-substituted phenyl ring. A number of π-alkyl interactions were observed. His266 was making a π-akyl interaction with the methyl group of the phenyl ring. Tyr275 was making a

Table 4
Binding free energies and non-bonded interactions of soybean 15-LOX inhibitors.

Ligand	Binding Free Energy (kJ/mol)	Hydrophobic interactions	Hydrogen bond interactions	Hydrogen bond distance (Å)	Other interactions and distance (Å)
7c	−20	Tyr275 (π-δ), Lys278 (alkyl), Phe272 (π-alkyl), Ala263 (π-alkyl), Leu273 (π-alkyl), Ala777 (π-alkyl), Ile857 (π-alkyl)	Lys278 (H-bond donor)	2.61 and 2.01	Asp553 (electrostatic, π-anion)
7d	−18	Ala263 (π-δ), Phe272 (π-alkyl), Val256 (π-alkyl), Leu563 (π-alkyl), Leu 273 (π-alkyl), Ala777 (π-alkyl), Ile857 (π-alkyl)	Lys278 (H-bond donor)	2.51	Asp553 (electrostatic, π-anion)
7f	−21	Val26 (alkyl), His266 (π-alkyl), Tyr275 (π-alkyl), Leu273 (π-alkyl), Ala263 (π-alkyl)	Thr274 (H-bond donor), Tyr275 (H-bond donor), Lys278 (H-bond donor), Asn556 (H-bond donor), His266 (H-bond donor)	2.1, 1.80 and 2.4, 2.71 and 2.4, 2.26, 2.8	Asp553 (electrostatic, π-anion), Phe272 (π-Sulfur)
7 g	−15	Tyr275 (π-π stacked), Lys278 (alkyl), Phe272 (π-alkyl), Tyr275 (π-alkyl), Ala263 (π-alkyl), Leu273 (π-alkyl), Ala777 (π-alkyl), Ile857 (π-alkyl)	Lys278 (H-bond donor)	2.53 and 2.20	Asp553 (electrostatic, π-anion)

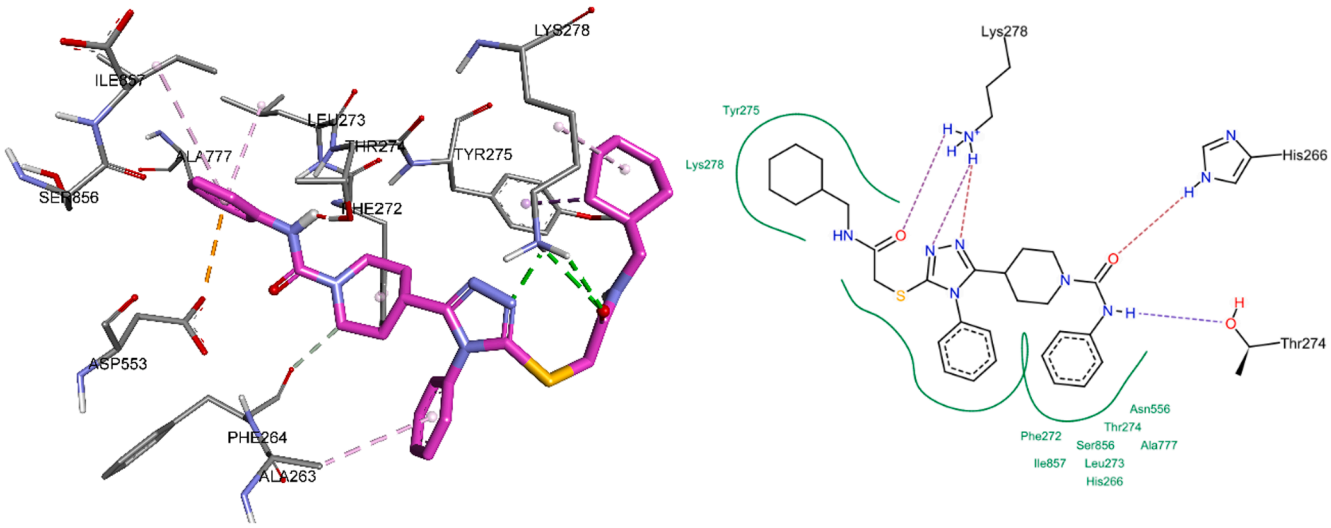

Fig. 3. Docked conformation of 15-LOX inhibitor **7c**.

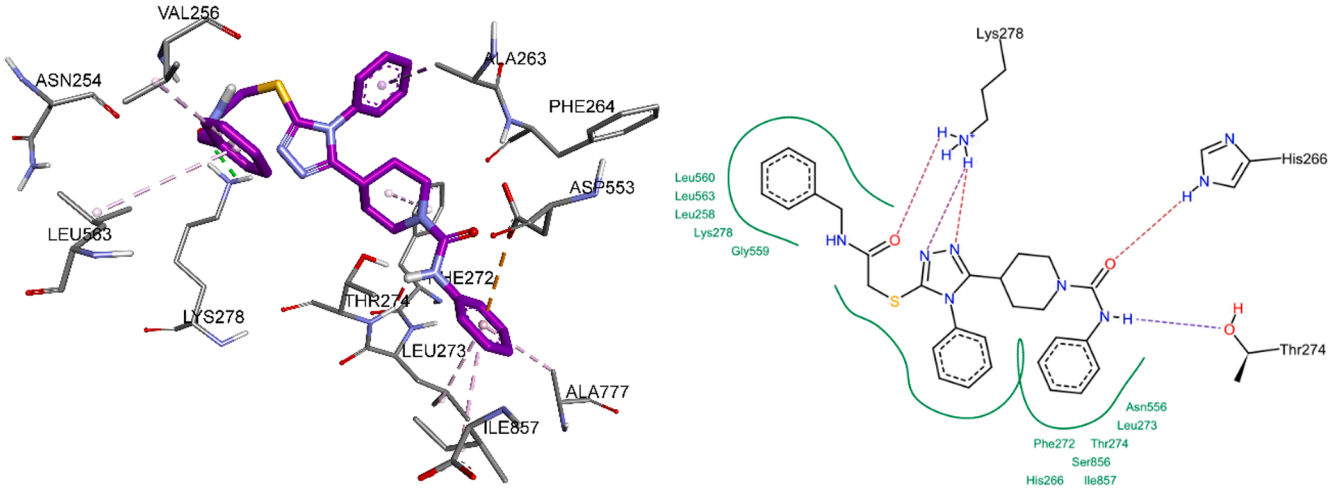

Fig. 4. Docked conformation of 15-LOX inhibitor **7d**.

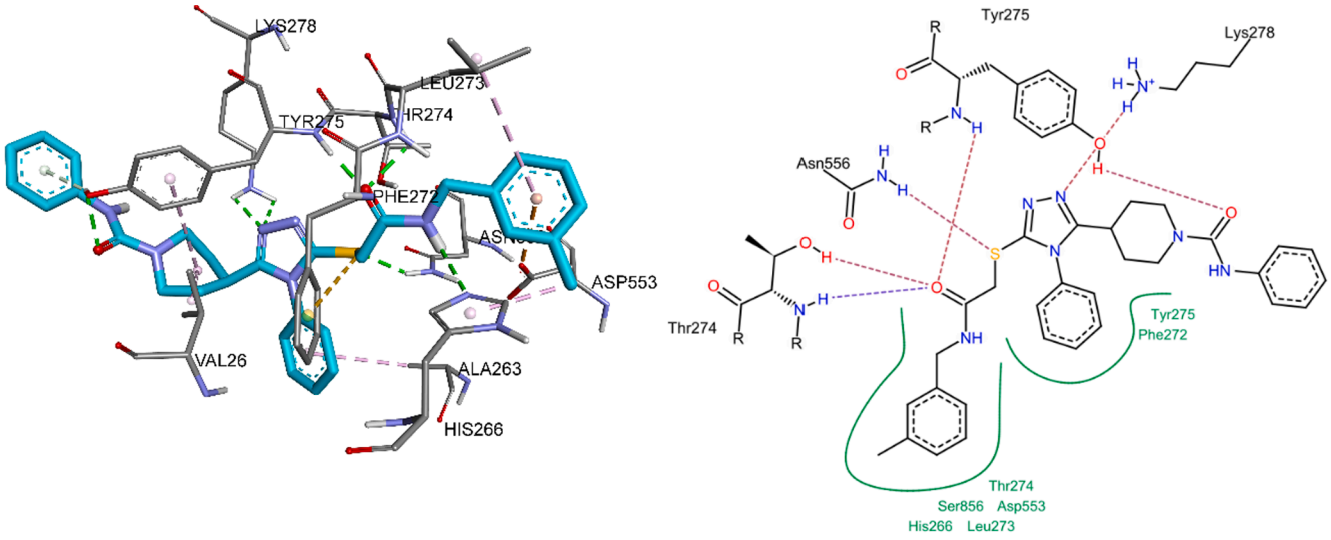

Fig. 5. Docked conformation of 15-LOX inhibitor **7f**.

π-alkyl interaction with the piperidine moiety. Leu273 was making a π-alkyl interaction with methyl substituted phenyl ring. Ala263 was making a π-alkyl interaction with the *N*-substituted phenyl ring.

The docked conformation of compound **7g** is shown in Fig. 6. Lys278 made hydrogen bonds with the nitrogen atom of the triazole ring. Asp553 was making a π-anion interaction with the phenyl ring connected to piperidinyl amide moiety. A π-π stacked interaction was observed between Tyr275 and ethyl substituted benzyl ring. Lys278 and Tyr 275 were making alkyl and π-alkyl interactions with the ethyl group of benzyl ring respectively. A number of hydrophobic π-alkyl interactions were observed. Phe272 was making a π-alkyl interaction with the piperidinyl ring. Ala263 was making a π-alkyl interaction with the *N*-substituted phenyl ring. Leu273, Ala777 and Ile857 were making π-alkyl interactions with the phenyl ring connected to piperidinyl amide moiety.

2.6. Molecular docking studies with human 5-LOX enzyme

Arachidonic acid is the substrate of 5-LOX, and is converted to leukotriene A4 (LTA4) which promotes inflammation. 5-LOX is also overexpressed in several types of cancers. Hence 5-LOX is an important drug target for anti-inflammatory and anti-cancer drugs. Therefore, the most active 15-LOX inhibitors were also docked against human 5-LOX. The crystal structure of the human 5-LOX enzyme in complex with its substrate, arachidonic acid, was downloaded from the PDB (PDB id: 3V99, 2.2 Å). Docking of the most active inhibitors was carried out (Table 5). All compounds were found to bind in the same area as that of arachidonic acid (Fig. 7).

The docked conformation of the most active inhibitor **7c** is shown in Fig. 8. One of the NH groups was making hydrogen bonds with Ala672, the carbonyl group adjacent to it was making a hydrogen bond with Asn554. The other NH group made a hydrogen bond with Gln363. The nitrogen atom of the triazole ring was making a hydrogen bond with Gln557. The phenyl group attached to the triazole ring made a π-δ interaction with Leu607.

Similar interactions were observed for **7f**, which had comparable inhibition to **7c**. Two different NH groups bind with Asn554 and Gln363, respectively, by separate hydrogen bonds. The nitrogen atoms of the triazole ring were making a hydrogen bond with Gln557. Furthermore, the sulfur atom was in direct contact with the iron atom of the enzyme's active site. The triazole ring was also making a π-δ interaction with His367, the toluene ring made a π-alkyl interaction with Leu607 (Fig. 9).

The docked conformations of the next most active inhibitors **7d** and **7g** are shown in Figs. 10, 11. They show mostly similar interactions, that is, one of the NH groups is making a hydrogen bond with Ala672, while the carbonyl group next to it is making a hydrogen bond with Asn554. The nitrogen atoms of the triazole ring made hydrogen bonds with Gln557. The sulfur atom was in direct contact with the active site's iron atom. The other NH group in compound **7d** was making a hydrogen bond with Gln363, while this interaction was absent for compound **7g**, this may in part, explain the difference in activity between the two.

One of the most striking feature observed, while comparing binding site interactions of soybean 15-LOX and human 5-LOX inhibitors, was that in case of human 5-LOX inhibition three out of five inhibitors indicated direct binding with the Fe^{2+} ion of the enzyme's active site. This metal–ligand interaction was not observed in case of soybean 15-LOX inhibitor. This leads us to speculate that the compounds described herein can be better inhibitors of 5-LOX over 15-LOX, and thus may have the potential to be developed further as potent anti-inflammatory agents.

3. Conclusion

In our endeavor to accomplish the design, synthesis, and characterization of new derivatives of 2-(4-phenyl-5-(1-phenylcarbamoyl)piperidine-4H-1,2,4-triazol-3-ylthio)acetamide (**7a-o**) as potential 15-LOX inhibitors, compounds **7c, 7f, 7d,** and **7g** are potent inhibitors against the enzyme and are less toxic with potential drug-likeness properties as determined by ADME studies. SAR reveals that both the position and nature of the substituent on the phenyl of acetamides are important for 15-LOX inhibition. In silico studies of revealed that the active molecules (**7c, 7f, 7d,** and **7g**) can be better inhibitors of 5-LOX over 15-LOX. Further investigations regarding stability under biological conditions and pharmacokinetic parameters are required which could be helpful to design more potent anti-inflammatory agents for therapeutic use.

4. Experimental

4.1. Materials and methods

All the chemicals and solvents of analytical grade were procured from Sigma, Aldrich, and Alfa Aesar, until unless specified. The ^{1}H and ^{13}C NMR spectra were recorded on Bruker instrument operating at 400 and 100 MHz, respectively, using tetramethylsilane as an internal standard. IR spectra were obtained on Shimadzu 460 FTIR spectrometer as KBr pellets. The mass spectra were measured on JMSA 500 mass spectrometer and JMS H × 110 spectrometer with a data system. Melting points were determined by using Gallen Kemp electrothermal apparatus.

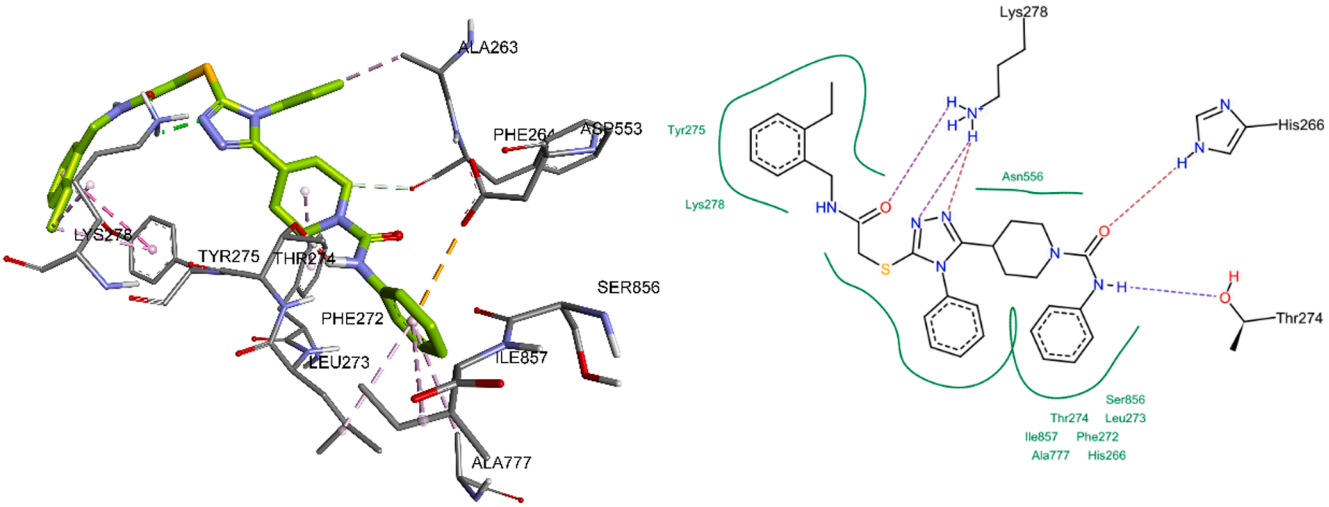

Fig. 6. Docked conformation of 15-LOX inhibitor **7g**.

Table 5
Binding free energies and non-bonded interactions of human 5-LOX inhibitors.

Ligand	Binding Free Energy (kJ/mol)	Hydrophobic interactions	Hydrogen bond interactions	Hydrogen bond distance (Å)	Other interactions and distance (Å)
7c	−20	Leu607 (*π*-*δ*), Ala672 (alkyl)	Ala672 (H-bond donor), Gln363 (H-bond donor), Asn554 (H-bond donor), Gln557 (H-bond donor)	1.8, 2.09, 2.09, 2.14	–
7d	−30	His367 (*π*-*δ*), Ala672 (*π*-alkyl)	Ala672 (H-bond donor), Gln363 (H-bond donor), Asn554 (H-bond donor)	1.72, 2.09, 2.06	Fe-ligand (2.39)
7f	−31	His367 (*π*-*δ*), Leu607 (*π*-alkyl)	Asn554 (H-bond donor), Gln363 (H-bond donor), Asn557 (H-bond donor)	2.09, 2.1, 2.05	Fe-ligand (2.37)
7g	–23	His367 (*π*-*δ*), Ala672 (*π*-*δ*), Ala410 (*π*-alkyl)	Ala672 (H-bond donor), Asn554 (H-bond donor), Asn557 (H-bond donor)	2.01, 2.09, 2.09	Fe-ligand (2.37)

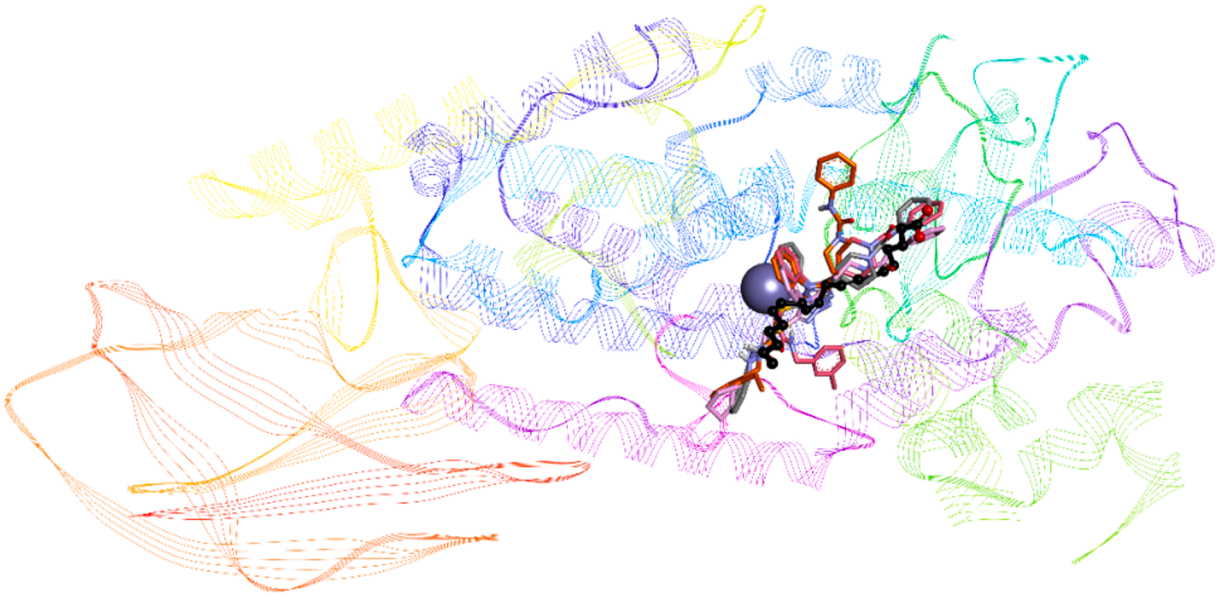

Fig. 7. Overlap of arachidonic acid (black) with 5-LOX inhibitors **7c** (light pink), **7d** (grey), **7f** (dark pink), and **7g** (orange). (For interpretation of the references to colour in this figure legend, the reader is referred to the web version of this article.)

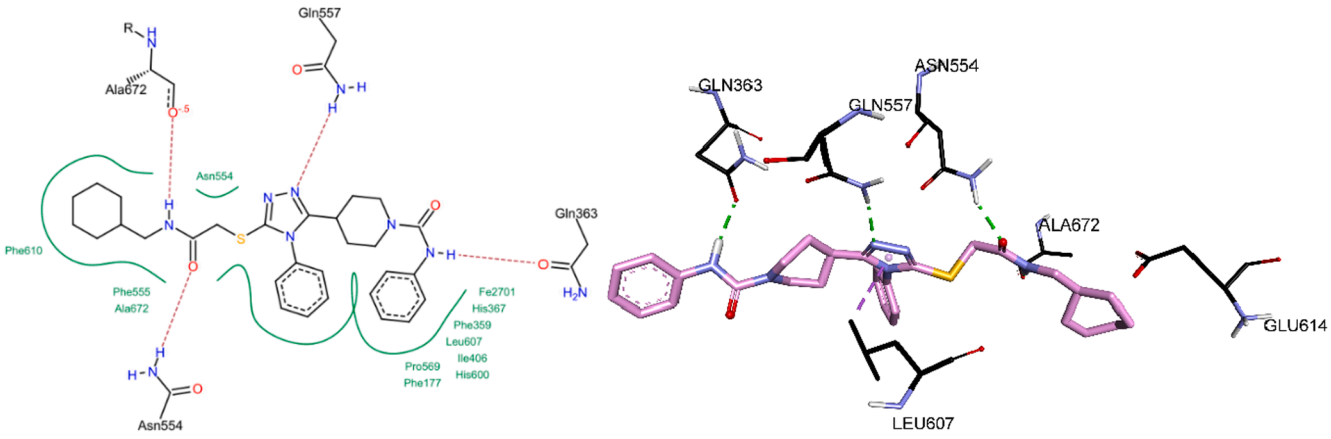

Fig. 8. Docked conformations of 5-LOX inhibitor **7c**.

4.2. Synthesis of ethyl 1-(phenylcarbamoyl)piperidine-4-carboxylate (1)

Ethyl piperidine-4-carboxylate (**a**; 0.025 mol, 3.8 mL) was taken in a watch glass and phenyl isocyanate (0.025 mol, 2.98 mL) was added drop wise with constant rubbing, which continued (15–20 min) till the appearance of a single spot on TLC. The physical and spectroscopic data of compound **1** is given below:

White solid; Yield: 98%; m.p. (105–108 °C); IR (KBr disk, cm^{-1}): 3396 (N—H), 3041 (Ar-H), 2950 (C—H), 1735, 1660 (C═O), 1615–1560 (Ar-C═C), 1260 (C—O, C—N); ^{1}H NMR (400 MHz, $CDCl_3$, ppm): δ 1.29 (3H, t, J = 7.0 Hz, $\underline{CH_3}$-CH_2-O), 1.89 (4H, m, H-3,5), 3.34 (1H, m, H-4), 3.39 (2H, m, H-2α,6α), 4.13 (2H, q, J = 7.0 Hz, CH_3-$\underline{CH_2}$-O), 4.34 (2H, br d, J = 13.2 Hz, H-2β,6β), 7.19 (1H, t, J = 7.5 Hz, H-4′), 7.43 (2H, t, J = 7.5 Hz, H-3′,5′), 7.61 (2H, d, J = 7.5 Hz, H-2′,6′); ^{13}C NMR (100 MHz, CD_3OD): δ 14.1 (CH_3), 28.5 (C-3,5), 40.4 (C-4), 46.5 (C-2,6), 62.1 (CH_2), 121.6 (C-2′,6′), 128.0 (C-4′), 128.9 (C-3′,5′), 139.4 (C-

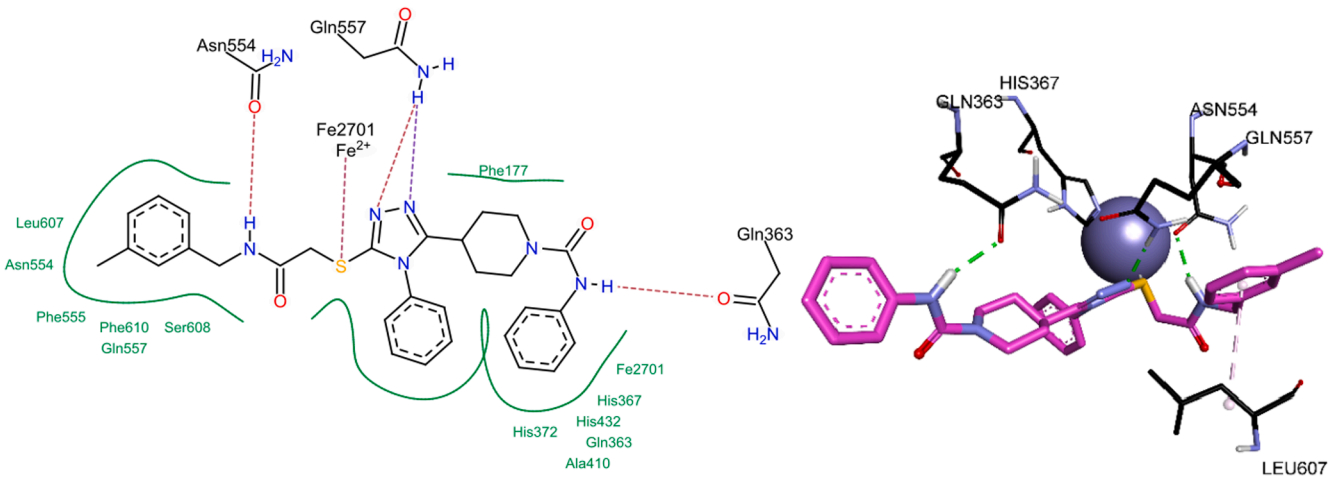

Fig. 9. Docked conformations of 5-LOX inhibitor **7f**.

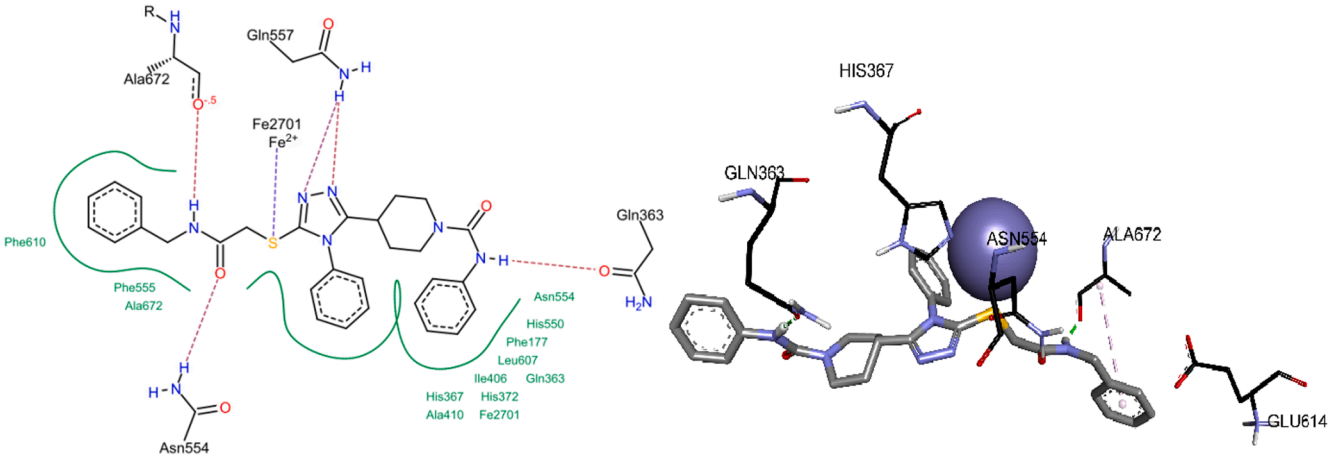

Fig. 10. Docked conformations of 5-LOX inhibitor **7d**.

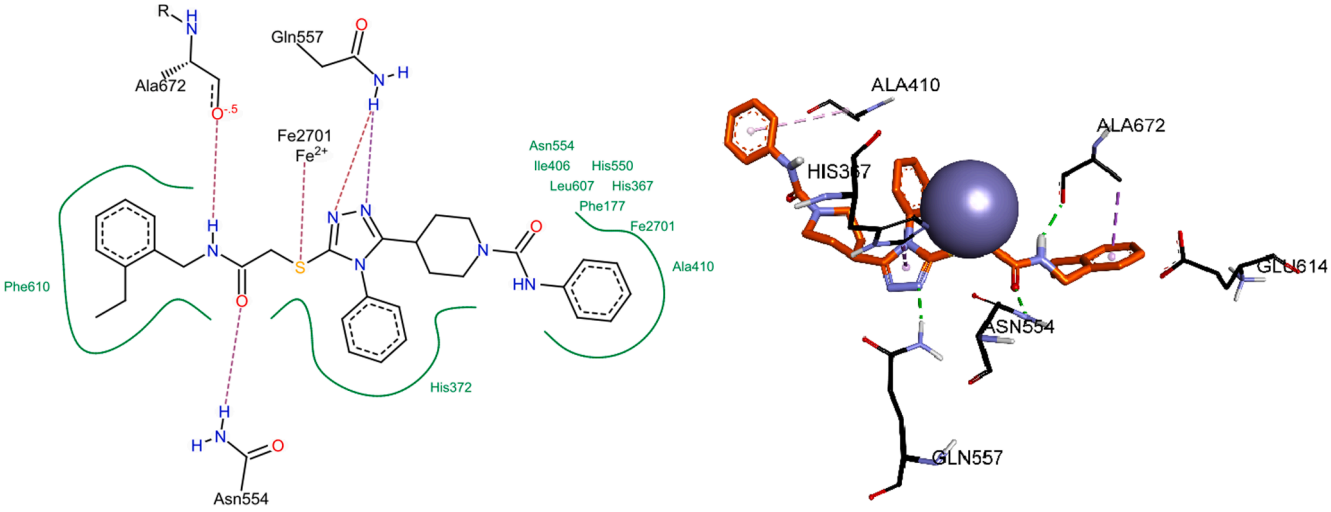

Fig. 11. Docked conformations of 5-LOX inhibitor **7g**.

1′), 158.1 (C═O), 175.8 (COOEt); HR-EI-MS (*m/z*): 276.1491 $[M]^+$ calculated for $C_{15}H_{20}N_2O_3$; 276.1473.

4.3. Synthesis of 4-(hydrazinecarbonyl)-N-phenylpiperidine-1-carboxamide (2)

In a 100 mL round bottom flask containing ethyl 1-

(phenylcarbamoyl)piperidine-4-carboxylate (**1**; 0.024 mol, 6.7 g), 30 mL of hydrazine hydrate (80%) was added slowly with constant stirring for 4–5 h. White fluffy precipitates were formed on cooling which were filtered, washed with cold distilled water and dried. The physical and spectroscopic data of **2** is as follows:

White shiny powder; Yield: 98%; m.p. (160–168 °C); IR (KBr disk, cm^{-1}): 3396, 3364 (N—H), 3040 (Ar-H), 2955 (C—H), 1680, 1660 (C═O), 1614–1561 (Ar-C═C), 1240 (C—N); ^{1}H NMR (400 MHz, $CDCl_3$, ppm): δ 1.87 (4H, m, H-3,5), 3.33 (1H, m, H-4), 3.39 (2H, m, H-2α,6α), 4.35 (2H, br d, J = 13.2 Hz, H-2β,6β), 7.19 (1H, t, J = 7.5 Hz, H-4′), 7.43 (2H, t, J = 7.5 Hz, H-3′,5′), 7.61 (2H, d, J = 7.5 Hz, H-2′,6′); ^{13}C NMR (100 MHz, CD_3OD): δ 29.4 (C-3,5), 40.1 (C-4), 47.0 (C-2,6), 121.6 (C-2′,6′), 128.0 (C-4′), 128.9 (C-3′,5′), 139.4 (C-1′), 158.1 (C═O), 178.2 (CONH); HR-EI-MS (*m/z*): 262.1449 $[M]^+$ calculated for $C_{13}H_{18}N_4O_2$; 262.1429.

4.4. Synthesis of N-phenyl-4-(2-(phenylcarbamothioyl) hydrazinecarbonyl)piperidine-1-carboxamide (3)

Phenyl isothiocyanate (2.63 mL, 0.022 mol) was added drop wise with stirring to a 100 mL round bottom flask already furnished with compound **2** (5.9 g, 0.022 mol) dissolved in 30 mL of methanol. The mixture was refluxed with stirring for 3–4 h and the precipitates were formed on cooling which were filtered, washed and dried. Below is the physical and spectroscopic data of **3**:

White powder; Yield: 98%; m.p. (180–183 °C); IR (KBr disk, cm^{-1}): 3364 (N—H), 3033 (Ar-H), 2939 (C—H), 1678, 1660 (C═O), 1617–1550 (Ar-C═C), 1215 (C—N); ^{1}H NMR (400 MHz, $CDCl_3$, ppm): δ 1.87 (4H, m, H-3,5), 3.34 (1H, m, H-4), 3.39 (2H, m, H-2α,6α), 4.35 (2H, br d, J = 13.2 Hz, H-2β,6β), 7.19 (1H, t, J = 7.5 Hz, H-4′), 7.25 (5H, br s, *N*-Ph), 7.43 (2H, t, J = 7.5 Hz, H-3′,5′), 7.61 (2H, d, J = 7.5 Hz, H-2′,6′); ^{13}C NMR (100 MHz, CD_3OD): δ 29.4 (C-3,5), 40.7 (C-4), 47.0 (C-2,6), 121.6 (C-2′,6′), 128.0 (C-4′), 128.9 (C-3′,5′), 139.4 (C-1′), *N*-Ph [126.6 (C-2,6), 128.4 (C-4), 129.0 (C-3,5), 138.5 (C-1)], 158.1 (C═O), 173.2 (CO), 181.1 (C═S); HR-EI-MS (*m/z*): 397.1593 $[M]^+$ calculated for $C_{20}H_{23}N_5O_2S$; 397.1572.

4.5. Synthesis of 4-(5-mercapto-4-phenyl-4H-1,2,4-triazol-3-yl)-N-phenylpiperdine-1-carboxamide (4)

Compound **3** (0.021 mol, 8.5 g) was dissolved in 10% aqueous NaOH (30 mL) in a 100 mL round bottom flask and was refluxed for 4 h. The reaction mixture was transferred into ice-cold water, acidified to pH 5–6 by using dilute HCl, precipitates were formed which were filtered, washed, and dried. The physical and spectroscopic data of **4** is as follows:

White powder; yield: 95%; m.p. (262–266 °C); IR (KBr disk, cm^{-1}): 3369 (N—H), 3031 (Ar-H), 2930 (C—H), 1661 (C═O), 1619–1560 (Ar-C═C, C═N), 1244 (C—N); ^{1}H NMR (400 MHz, $CDCl_3$, ppm): δ 1.92 (4H, m, H-3′,5′), 3.35 (1H, m, H-4′), 3.39 (4H, m, H-2a′,6a′), 4.33 (2H, br d, J = 13.2 Hz, H-2b′,6b′), 7.19 (1H, t, J = 7.5 Hz, H-4″), 7.43 (2H, t, J = 7.5 Hz, H-3″,5″), 7.61 (2H, d, J = 7.5 Hz, H-2″,6″), *N*-Ph [7.41 (2H, m, H-2,6), 7.60 (3H, m, H-3–5)]; ^{13}C NMR (100 MHz, CD_3OD): δ 29.4 (C-3′,5′), 40.7 (C-4′), 47.0 (C-2′,6′), 121.6 (C-2″,6″), 128.0 (C-4″), 128.9 (C-3″,5″), 139.4 (C-1″), *N*-Ph [126.6 (C-2,6), 128.4 (C-4), 129.0 (C-2,5), 138.5 (C-1)], 158.1 (C═O), 173.2 (C═O), 181.1 (C═S). HR-EI-MS (*m/z*): 379.1451 $[M]^+$ calculated for $C_{20}H_{21}N_5OS$; 379.1466.

4.6. General procedure for the synthesis of compounds 6a-o

Computed amounts of alkyl/aralkyl/aryl amines (**5a-o**, 0.01 mol) were added separately in a quick fit Erlenmeyer flask already having 20% aqueous Na_2CO_3 solution to set the pH 9–10. The bromoacetyl bromide (0.01 mol) was added drop-wise into the flask over 2–5 min with continuous vigorous shaking till the formation of precipitates followed by further stirring to get homogenous precipitates over a period of 1–2 h. The solid product was filtered, washed with cold water, and dried to get the respective electrophile(s), *N*-alkyl/aralkyl/aryl substituted-2-bromoacetamides (**6a-o**) and their names and physic-chemical constants are as follows:

4.6.1. 2-Bromo-N,N-diethylacetamide (6a)

Colorless liquid; Pungent smell; Yield: 98%; B.P.: 217-219℃; Solubility (CH_3OH).

4.6.2. 2-Bromo-N-propylacetamide (6b)

Colorless liquid; Pungent smell; Yield: 99%; B.P.: 201-206℃; Solubility (CH_3OH).

4.6.3. 2-Bromo-N-(cyclohexylmethyl)acetamide (6c)

White amorphous powder; Odorless Yield: 99%; M.P.: 98-100℃; Solubility (CH_3OH).

4.6.4. 2-Bromo N-benzylacetamide (6d)

White amorphous powder; Odorless; Yield: 97%; M.P.: 122-124℃; Solubility (CH_3OH).

4.6.5. 2-Bromo-N-(o-tolyl)acetamide (6e)

White amorphous powder; Odorless; Yield: 99%; M.P.: 107-110℃; Solubility (CH_3OH).

4.6.6. 2-Bromo-N-(m-tolyl)acetamide (6f)

Pink amorphous powder; Odorless; Yield: 99%; M.P.: 104-106℃; Solubility (CH_3OH).

4.6.7. 2-Bromo-N-(2-ethylphenyl)acetamide (6g)

White amorphous powder; Odorless; Yield: 99%; M.P.: 90-91℃; Solubility (CH_3OH).

4.6.8. 2-Bromo-N-(4-ethylphenyl)acetamide (6h)

Yellow amorphous powder; Odorless; Yield: 92%; M.P.: 118-119℃; Solubility (CH_3OH).

4.6.9. 2-Bromo-N-(2,3-dimethylphenyl)acetamide (6i)

White amorphous powder; Odorless; Yield: 99%; M.P.: 123-125 C; Solubility (CH_3OH).

4.6.10. 2-Bromo-N-(2,4-dimethylphenyl)acetamide (6j)

Off white amorphous powder; Odorless; 99%; M.P.: 150-153 ℃; Solubility (CH_3OH).

4.6.11. 2-Bromo-N-(2,5-dimethylphenyl)acetamide (6k)

White amorphous powder; Odorless; 99%; M.P.: 138-140 C; Solubility (CH_3OH).

4.6.12. 2-Bromo-N-(2,6-dimethylphenyl)acetamide (6l)

White amorphous powder; Odorless; Yield: 99%; M.P.: 140-143 C; Solubility (CH_3OH).

4.6.13. 2-Bromo-N-(3,4-dimethylphenyl)acetamide (6m)

Yellow amorphous powder; Odorless; 93%; M.P.: 127-129 C; Solubility (CH_3OH).

4.6.14. 2-Bromo-N-(3,5-dimethylphenyl)acetamide (6n)

Yellow amorphous powder; Odorless; 90%; M.P.: 124-126 C; Solubility (CH_3OH).

4.6.15. 2-Bromo-N-phenylacetamide (6o)

White amorphous powder; Odorless; Yield: 99%; M.P.: 112-115 C; Solubility (CH_3OH).

4.7. General method for the synthesis of compounds **7a-o**

In a 50 mL round bottom flask, 0.2 g (0.5 mmol) of compound **4** was dissolved in methanol (5 mL) and 30 mL ethanolic KOH (0.5 mmol) was added and the mixture was stirred for 30 min at room temperature. The electrophiles (**6a-o**) separately were added slowly to the mixture and set to reflux for 4–5 h. An excess amount of cold distilled water was added and the precipitates of the final products, **7a-o**, were formed separately, which were filtered, washed, and dried.

4.7.1. 4-(5-(2-(Diethylamino)-2-oxoethylthio)-4-phenyl-4H-1,2,4-triazol-3-yl)-N-phenylpiperidine-1-carboxamide (7a)

White amorphous powder; Yield: 93%; M.P.: 98-100 ℃; IR (KBr) ν_{max}: 3365 (N—H), 3045 (Ar-H), 2941 (C—H), 1681, 1662 (C═O), 1619–1544 (Ar-C═C, C═N), 1260 (C—N); ^{1}H NMR (400 MHz, CD_3OD): δ 1.10 (2H, t, J = 7.1 Hz, H-2‴), 1.22 (2H, t, J = 7.1 Hz, H-2⁗), 1.81 (4H, m, H-3′,5′), 2.80 (1H, m, H-4′), 2.84 (2H, m, H-2α′,6α′), 3.35 (2H, q, J = 7.1 Hz, H-1‴), 3.45 (2H, q, J = 7.1 Hz, H-1⁗), 4.15 (2H, br d, J = 13.2 Hz, H-2β′,6β′), 4.17 (2H, s, H-2‴), 7.00 (1H, t, J = 7.5 Hz, H-4″), 7.24 (2H, t, J = 8.0 Hz, H-3″,5″), 7.32 (2H, d, J = 7.5 Hz, H-2″,6″), *N*-Ph [7.48 (2H, m, H-2,6), 7.64 (3H, m, H-3–5)]; ^{13}C NMR (100 MHz, CD_3OD): δ 11.7 (C-2⁗), 13.0 (C-2⁗), 29.9 (C-3′,5′), 32.8 (C-4′), 35.4 (C-2‴), 40.7 (C-1‴), 42.5 (C-1⁗), 43.5 (C-2′,6′), 120.8 (C-2″,6″), 122.7 (C-4″), 128.2 (C-3″,5″), *N*-Ph [127.5 (C-2,6), 130.0 (C-3,5), 130.4 (C-4), 132.8 (C-1)], 139.6 (C-1″), 151.4 (C-3), 156.4 (C═O), 158.7 (C-5), 166.8 (C-1‴); HR-EI-MS (*m/z*): 442.2330 $[M]^+$ calculated for $C_{26}H_{32}N_6O_2S$; 442.2307.

4.7.2. 4-(5-(2-Oxo-2-(propylamino)ethylthio)-4-phenyl-4H-1,2,4-triazol-3-yl)-N-phenylpiperidine-1-carboxamide (7b)

White amorphous powder; Yield: 95%; M.P.: 115-120℃; IR (KBr) ν_{max}: 3360 (N—H), 3035 (Ar-H), 2951 (C—H), 1680, 1660 (C═O), 1620–1540 (Ar-C═C, C═N), 1261 (C—N); ^{1}H NMR (400 MHz, CD_3OD): δ 0.89 (3H, t, J = 7.0 Hz, H-3⁗), 1.50 (2H, sexet, J = 7.0 Hz, H-2⁗), 1.80 (4H, m, H-3′,5′), 2.81 (1H, m, H-4′), 2.84 (2H, m, H-2α′,6α′), 3.13 (2H, t, J = 7.0 Hz, H-1⁗), 3.83 (2H, s, H-2‴), 4.15 (2H, br d, J = 13.2 Hz, H-2β′,6β′), 7.00 (1H, t, J = 8.0 Hz, H-4″), 7.24 (2H, t, J = 8.0 Hz, H-3″,5″), 7.32 (2H, d, J = 8.0 Hz, H-2″,6″), *N*-Ph [7.46 (2H, m, H-2,6), 7.64 (3H, m, H-3–5)]; ^{13}C NMR (100 MHz, CD_3OD): δ 11.7 (C-3⁗), 23.5 (C-2⁗), 31.2 (C-3′,5′), 34.2 (C-4′), 36.7 (C-2‴), 42.7 (C-1⁗), 45.0 (C-2′,6′), 122.2 (C-2″,6″), 124.1 (C-4″), 129.5 (C-3″,5″), *N*-Ph [128.8 (C-2,6), 131.4 (C-3,5), 131.8 (C-4), 134.1 (C-1)], 140.9 (C-1″), 152.6 (C-3), 157.8 (C═O), 160.2 (C-5), 169.8 (C-1‴); HR-EI-MS (*m/z*): 478.2169 $[M]^+$ calculated for $C_{25}H_{30}N_6O_2S$; 478.2150.

4.7.3. 4-(5-(2-(Cyclohexylamino)-2-oxoethylthio)-4-phenyl-4H-1,2,4-triazol-3-yl)-N-phenylpiperidine-1-carboxamide (7c)

White amorphous powder; Yield: 93%; M.P.: 210-220 ℃; IR (KBr) ν_{max}: 3351 (N—H), 3033 (Ar-H), 2955 (C—H), 1681, 1665 (C═O), 1625–1540 (Ar-C═C, C═N), 1260 (C—N); ^{1}H NMR (400 MHz, CD_3OD): δ 1.19 (2H, m, H-3⁗,5⁗), 1.31 (4H, m, H-2⁗,6⁗), 1.34 (2H, m, H-4⁗), 1.59 (1H, m, H-1⁗), 1.70 (2H, m, H-3⁗,5⁗), 1.79 (4H, m, H-3′,5′), 2.76 (1H, m, H-4′), 2.80 (2H, m, H-2α′,6α′), 3.61 (2H, t, J = 7.0 Hz, H-1⁗), 3.77 (2H, s, H-2‴), 4.15 (2H, br d, J = 13.2 Hz, H-2β′,6β′), 6.98 (1H, t, J = 8.0 Hz, H-4″), 7.22 (2H, t, J = 8.0 Hz, H-3″,5″), 7.29 (2H, d, J = 8.0 Hz, H-2″,6″), *N*-Ph [7.33 (2H, m, H-2,6), 7.61 (3H, m, H-3–5)]; ^{13}C NMR (100 MHz, $CDCl_3$ + CD_3OD): δ 25.3 (C-2⁗,6⁗), 26.1 (C-4⁗), 30.1 (C-3⁗,5⁗), 33.0 (C-1⁗), 33.0 (C-3′,5′), 33.6 (C-4′), 36.4 (C-2‴), 44.4 (C-2′,6′), 121.7 (C-2″,6″), 123.7 (C-4″), 129.2 (C-3″,5″), *N*-Ph [128.1 (C-2,6), 131.0 (C-3,5), 131.5 (C-4), 133.3 (C-1)], 140.2 (C-1″), 152.4 (C-3), 157.2 (C═O), 159.4 (C-5), 168.1 (C-1‴); HR-EI-MS (*m/z*): 518.2483 $[M]^+$ calculated for $C_{29}H_{36}N_6O_2S$; 518.2463.

4.7.4. 4-(5-(2-(Benzylamino)-2-oxoethylthio)-4-phenyl-4H-1,2,4-triazol-3-yl)-N-phenylpiperidine-1-carboxamide (7d)

White amorphous powder; Yield: 93%; M.P.: 195-200 ℃; IR (KBr) ν_{max}: 3355 (N—H), 3039 (Ar-H), 2957 (C—H), 1682, 1661 (C═O), 1622–1540 (Ar-C═C, C═N), 1261 (C—N); ^{1}H NMR (400 MHz, CD_3OD): δ 1.82 (4H, m, H-3′,5′), 2.75 (1H, m, H-4′), 2.79 (2H, m, H-2α′,6α′), 3.87 (2H, s, H-2‴), 4.13 (2H, br d, J = 13.2 Hz, H-2β′,6β′), 4.36 (2H, s, H-7⁗), 6.98 (1H, t, J = 8.0 Hz, H-4″), 7.22 (5H, m, H-2⁗-6⁗), 7.24 (2H, t, J = 8.0 Hz, H-3″,5″), 7.32 (2H, d, J = 8.0 Hz, H-2″,6″), *N*-Ph [7.34 (2H, m, H-2,6), 7.60 (3H, m, H-3–5)]; ^{13}C NMR (100 MHz, $CDCl_3$ + CD_3OD): δ 30.6 (C-3′,5′), 33.6 (C-4′), 36.1 (C-2‴), 44.3 (C-7⁗), 44.4 (C-2′,6′), 121.7 (C-2″,6″), 123.7 (C-4″), 127.9 (C-4⁗), 128.0 (C-3″,5″), 129.1 (C-2⁗,3⁗,5⁗,6⁗), *N*-Ph [127.9 (C-2,6), 131.0 (C-3,5), 131.5 (C-4), 133.2 (C-1)], 138.6 (C-2⁗), 140.1 (C-1″), 152.0 (C-3), 157.1 (C═O), 159.0 (C-5), 169.1 (C-1‴); HR-EI-MS (*m/z*): 526.2169 $[M]^+$ calculated for $C_{29}H_{30}N_6O_2S$; 526.2150.

4.7.5. 4-(5-(2-Oxo-2-(2-methylphenylamino)ethylthio)-4-phenyl-4H-1,2,4-triazol-3-yl)-N-phenylpiperidine-1-carboxamide (7e)

White amorphous powder; Yield: 88%; M.P.: 176-180 ℃; IR (KBr) ν_{max}: 3354 (N—H), 3038 (Ar-H), 2951 (C—H), 1680, 1664 (C═O), 1621–1530 (Ar-C═C, C═N), 1260 (C—N); ^{1}H NMR (400 MHz, CD_3OD): δ 1.82 (4H, m, H-3′,5′), 2.76 (1H, m, H-4′), 2.22 (3H, s, CH_3), 2.81 (2H, m, H-2α′,6α′), 4.02 (2H, s, H-2‴), 4.15 (2H, br d, J = 13.2 Hz, H-2β′,6β′), 6.98 (1H, t, J = 8.5 Hz, H-4″), 7.06 (1H, d, J = 8.5 Hz, H-6⁗), 7.16 (1H, t, J = 8.5 Hz, H-5⁗), 7.19 (1H, t, J = 8.5 Hz, H-4⁗), 7.22 (2H, t, J = 8.5 Hz, H-3″,5″), 7.30 (2H, d, J = 8.5 Hz, H-2″,6″), 7.49 (1H, t, J = 8.5 Hz, H-3⁗), *N*-Ph [7.37 (2H, m, H-2,6), 7.61 (3H, m, H-3–5)]; ^{13}C NMR (100 MHz, $CDCl_3$ + CD_3OD): δ 18.2 (CH_3), 30.7 (C-3′,5′), 33.7 (C-4′), 36.1 (C-2‴), 44.5 (C-2′,6′), 121.8 (C-2″,6″), 123.8 (C-4″), 125.2 (C-6⁗), 126.8 (C-3⁗), 127.0 (C-4⁗), 129.2 (C-3″,5″), 131.2 (C-5⁗), 132.4 (C-2⁗), *N*-Ph [128.1 (C-2,6), 131.1 (C-3,5), 131.6 (C-4), 133.3 (C-1)], 136.1 (C-1⁗), 140.2 (C-1″), 152.6 (C-3), 157.2 (C═O), 159.7 (C-5), 168.2 (C-1‴); HR-EI-MS (*m/z*): 526.2170 $[M]^+$ calculated for $C_{29}H_{30}N_6O_2S$; 526.2150.

4.7.6. 4-(5-(2-Oxo-2-(3-methylphenylamino)ethylthio)-4-phenyl-4H-1,2,4-triazol-3-yl)-N-phenylpiperidine-1-carboxamide (7f)

White amorphous powder; Yield: 89%; M.P.: 127-130℃; IR (KBr) ν_{max}: 3350 (N—H), 3035 (Ar-H), 2950 (C—H), 1681, 1661 (C═O), 1619–1525 (Ar-C═C, C═N), 1262 (C—N); ^{1}H NMR (400 MHz, CD_3OD): δ 1.85 (4H, m, H-3′,5′), 2.31 (3H, s, CH_3), 2.79 (1H, m, H-4′), 2.83 (2H, m, H-2α′,6α′), 3.73 (2H, s, H-2‴), 4.16 (2H, br d, J = 13.2 Hz, H-2β′,6β′), 6.92 (1H, d, J = 7.5 Hz, H-6⁗), 6.99 (1H, t, J = 7.5 Hz, H-4″), 7.17 (1H, t, J = 7.5 Hz, H-5⁗), 7.23 (2H, t, J = 8.0 Hz, H-3″,5″), 7.31 (2H, d, J = 7.5 Hz, H-2″,6″), 7.33 (1H, d, J = 7.5 Hz, H-4⁗), 7.35 (1H, s, H-2⁗), *N*-Ph [7.43 (2H, m, H-2,6), 7.60 (3H, m, H-3–5)]; ^{13}C NMR (100 MHz, $CDCl_3$ + CD_3OD): δ 21.6 (CH_3), 31.0 (C-3′,5′), 33.2 (C-4′), 34.1 (C-2‴), 44.8 (C-2′,6′), 118.1 (C-2⁗), 121.5 (C-6⁗), 122.1 (C-2″,6″), 124.0 (C-4″), 126.1 (C-4⁗), 129.4 (C-3″,5″), 129.6 (C-5⁗), *N*-Ph [128.6 (C-2,6),131.3 (C3,5), 131.7 (C-4), 133.9 (C-1)], 139.2 (C-3⁗), 139.7 (C-1⁗), 140.7 (C-1″), 152.5 (C-3), 157.6 (C═O), 160.1 (C-5), 167.8 (C-1‴); HR-EI-MS (*m/z*): 526.2170 $[M]^+$ calculated for $C_{29}H_{30}N_6O_2S$; 526.2150.

4.7.7. 4-(5-(2-(2-Ethylphenylamino)-2-oxoethylthio)-4-phenyl-4H-1,2,4-triazol-3-yl)-N-phenylpiperidine-1-carboxamide (7g)

White amorphous powder; Yield: 91%; M.P.: 95-105℃; IR (KBr) ν_{max}: 3352 (N—H), 3031 (Ar-H), 2951 (C—H), 1680, 1663 (C═O), 1618–1519 (Ar-C═C, C═N), 1260 (C—N); ^{1}H NMR (400 MHz, CD_3OD): δ 1.13 (3H, t, J = 7.2 Hz, $\underline{CH_3}$-CH_2), 1.84 (4H, m, H-3′,5′), 2.59 (2H, q, J = 7.2 Hz, CH_3-$\underline{CH_2}$), 2.79 (1H, m, H-4′), 2.84 (2H, m, H-2α′,6α′), 4.06 (2H, s, H-2‴), 4.15 (2H, br d, J = 13.2 Hz, H-2β′,6β′), 6.99 (1H, t, J = 7.5 Hz, H-4″), 7.17 (2H, m, H-4⁗,6⁗), 7.23 (2H, t, J = 8.0 Hz, H-3″,5″), 7.25 (1H, t, J = 8.0 Hz, H-5⁗), 7.32 (2H, d, J = 8.0 Hz, H-2″,6″), 7.38 (1H, d, J = 7.5 Hz, H-3⁗), *N*-Ph [7.46 (2H, m, H-2,6), 7.63 (3H, m, H-3–5)]; ^{13}C NMR (100 MHz, CD_3OD): δ 14.9 (CH_3), 26.2 (CH_2), 31.2 (C-3′,5′), 34.2 (C-4′), 37.0 (C-2‴), 44.9 (C-2′,6′), 122.2 (C-2″,6″), 124.1 (C-4″), 127.0 (C-6⁗), 127.3 (C-4⁗), 127.8 (C-3⁗), 129.9 (C-5⁗), 129.5 (C-3″,5″), *N*-Ph [128.8 (C-2,6), 131.4 (C-3,5), 131.9 (C-4), 134.0 (C-1)], 135.9 (C-2⁗), 139.8 (C-1⁗), 140.9 (C-1″), 152.8 (C-3), 157.7 (C═O),

160.4 (C-5), 169.2 (C-1‴); HR-EI-MS (*m/z*): 540. 2325 $[M]^+$ calculated for $C_{30}H_{32}N_6O_2S$; 540.2307.

*4.7.8. 4-(5-(2-(4-Ethylphenylamino)-2-oxoethylthio)-4-phenyl-4H-1,2,4-triazol-3-yl)-N-phenylpiperidine-1-carboxamide (**7h**)*

White amorphous powder; Yield: 96%; M.P.: 100-104 ℃; IR (KBr) ν_{max}: 3351 (N—H), 3036 (Ar-H), 2961 (C—H), 1683, 1661 (C═O), 1617–1517 (Ar-C═C, C═N), 1261 (C—N); ^{1}H NMR (400 MHz, CD_3OD): δ 1.18 (3H. t, J = 7.5 Hz, $\underline{CH_3}$-CH_2), 1.80 (4H, m, H-3′,5′), 2.58 (2H, q, J = 7.5 Hz, CH_3-$\underline{CH_2}$), 2.74 (1H, m, H-4′), 2.79 (2H, m, H-2α′,6α′), 3.96 (2H, s, H-2‴), 4.13 (2H, br d, J = 13.2 Hz, H-2β′,6β′), 6.98 (1H, t, J = 8.0 Hz, H-4″), 7.11 (2H, d, J = 8.0 Hz, H-2⁗,6⁗), 7.22 (2H, t, J = 8.0 Hz, H-3″,5″), 7.32 (2H, d, J = 8.0 Hz, H-2″,6″), 7.42 (2H, t, J = 8.0 Hz, H-3⁗,5⁗), *N*-Ph [7.35 (2H, m, H-2,6), 7.59 (3H, m, H-3–5)]; ^{13}C NMR (100 MHz, $CDCl_3$ + CD_3OD): δ 16.0 (CH_3), 28.8 (CH_2), 30.5 (C-3′,5′), 34.0 (C-2‴), 33.5 (C-4′), 37.1 (C-2‴), 44.3 (C-2′,6′), 120.7 (C-2⁗,6⁗), 121.5 (C-2″,6″), 123.6 (C-4″), 128.7 (C-3⁗,5⁗), 129.1 (C-3″,5″), *N*-Ph [(127.9 (C2,6), 130.9 (C-3,5), 131.5 (C-4), 133.0 (C-1)], 136.2 (C-4⁗), 140.0 (C-1⁗), 141.3 (C-1″), 152.6 (C-3), 157.0 (C═O), 159.4 (C-5), 167.0 (C-1‴); HR-EI-MS (*m/z*): 540.2325 $[M]^+$ calculated for $C_{30}H_{32}N_6O_2S$; 540.2307.

*4.7.8.1. 4-(5-(2-(2,3-Dimethylphenylamino)-2-oxoethylthio)-4-phenyl-4H-1,2,4-triazol-3-yl)-N-phenylpiperidine-1-carboxamide (**7i**).* White amorphous powder; Yield: 93%; M.P.: 160-167 ℃; IR (KBr) ν_{max}: 3355 (N—H), 3039 (Ar-H), 2965 (C—H), 1682, 1664 (C═O), 1615–1515 (Ar-C═C, C═N), 1260 (C—N); ^{1}H NMR (400 MHz, CD_3OD): δ 1.83 (4H, m, H-3′,5′), 2.11 (3H, s, CH_3), 2.29 (3H, s, CH_3), 2.80 (1H, m, H-4′), 2.84 (4H, m, H-2α′,6α′), 4.05 (2H, s, H-2‴), 4.17 (2H, br d, J = 13.2 Hz, H-2β′,6β′), 7.00 (1H, t, J = 8.0 Hz, H-4″), 7.05 (2H, d, J = 8.0 Hz, H-4⁗,6⁗), 7.15 (1H, t, J = 8.0 Hz, H-5⁗), 7.24 (2H, t, J = 8.0 Hz, H-3″,5″), 7.32 (1H, d, J = 8.0 Hz, H-2″,6″), *N*-Ph [7.47 (2H, m, H-2,6), 7.64 (3H, m, H-3–5)]; ^{13}C NMR (100 MHz, CD_3OD): δ 14.3 (CH_3), 20.5 (CH_3), 31.2 (C-3′,5′), 34.2 (C-4′), 37.1 (C-1‴), 44.9 (C-2′,6′), 122.2 (C-2″,6″), 124.1 (C-4″), 124.6 (C-6⁗), 126.6 (C-4⁗), 129.1 (C-5⁗), 129.5 (C-3″,5″), 133.0 (C-3⁗), 134.1 (C-2⁗), *N*-Ph [128.9 (C-2,6), 131.4 (C-3,5), 131.8 (C-4), 136.4 (C-1)], 138.8 (C-1⁗), 140.9 (C-1″), 152.7 (C-3), 157.8 (C═O), 160.4 (C-5), 168.9 (C-1‴); HR-EI-MS (*m/z*): 540.2325 $[M]^+$ calculated for $C_{30}H_{32}N_6O_2S$; 540.2307.

*4.7.8.2. 4-(5-(2-(2,4-Dimethylphenylamino)-2-oxoethylthio)-4-phenyl-4H-1,2,4-triazol-3-yl)-N-phenylpiperidine-1-carboxamide (**7j**).* White amorphous powder; Yield: 92%; M.P.: 90-100 ℃; IR (KBr) ν_{max}: 3351 (N—H), 3041 (Ar-H), 2969 (C—H), 1681, 1661 (C═O), 1611–1513 (Ar-C═C, C═N), 1261 (C—N); ^{1}H NMR (400 MHz, CD_3OD): δ 1.82 (4H, m, H-3′,5′), 2.17 (3H, s, CH_3), 2.26 (3H, s, CH_3), 2.78 (1H, m, H-4′), 2.81 (2H, m, H-2α′,6α′), 4.00 (2H, s, H-2‴), 4.15 (2H, br d, J = 13.2 Hz, H-2β′,6β′), 6.97 (1H, t, J = 8.0 Hz, H-4″), 7.00 (1H, d, J = 8.0 Hz, H-6⁗), 7.03 (1H, s, H-3⁗), 7.23 (2H, t, J = 8.0 Hz, H-3″,5″), 7.30 (3H, d, J = 8.0 Hz, H-2″,6″), 7.33 (1H, d, J = 8.0 Hz, H-5⁗), *N*-Ph [7.38 (2H, m, H-2,6), 7.61 (3H, m, H-3–5)]; ^{13}C NMR (100 MHz, $CDCl_3$ + CD_3OD): δ 18.1 (CH_3), 21.0 (CH_3), 30.8 (C-3′,5′), 33.8 (C-4′), 36.7 (C-1‴), 44.5 (C-2′,6′), 121.8 (C-2″,6″), 123.8 (C-4″), 125.4 (C-6⁗), 127.6 (C-3⁗), 129.2 (C-3″,5″), 131.6 (C-5⁗), 133.4 (C-4⁗), *N*-Ph [128.2 (C-2,6), 131.2 (C-3,5), 131.9 (C-4), 133.5 (C-1)], 133.4 (C-4⁗), 133.6 (C-2⁗), 136.7 (C-1⁗), 140.3 (C-1″), 152.6 (C-3), 157.3 (C═O), 159.8 (C-5), 168.3 (C-1‴); HR-EI-MS (*m/z*): 540.2325 $[M]^+$ calculated for $C_{30}H_{32}N_6O_2S$; 540.2307.

*4.7.8.3. 4-(5-(2-(2,5-Dimethylphenylamino)-2-oxoethylthio)-4-phenyl-4H-1,2,4-triazol-3-yl)-N-phenylpiperidine-1-carboxamide (**7k**).* White amorphous powder; Yield: 92%; M.P.: 175-180 ℃; IR (KBr) ν_{max}: 3353 (N—H), 3044 (Ar-H), 2967 (C—H), 1682, 1660 (C═O), 1612–1514 (Ar-C═C, C═N), 1262 (C—N); ^{1}H NMR (400 MHz, CD_3OD): δ 1.84 (4H, m, H-3′,5′), 2.17 (3H, s, CH_3), 2.26 (3H, s, CH_3), 2.77 (1H, m, H-4′), 2.81 (2H, m, H-2α′,6α′), 4.01 (2H, s, H-2‴), 4.14 (2H, br d, J = 13.2 Hz, H-2β′,6β′), 6.90 (1H, d, J = 7.6 Hz, H-4⁗), 6.98 (1H, t, J = 8.0 Hz, H-4″), 7.05 (1H, d, J = 7.6 Hz, H-3⁗), 7.22 (2H, t, J = 8.0 Hz, H-3″,5″), 7.30 (2H, d, J = 8.0 Hz, H-2″,6″), 7.32 (1H, s, H-6⁗), *N*-Ph [7.37 (2H, m, H-2,6), 7.61 (3H, m, H-3,5)]; ^{13}C NMR (100 MHz, $CDCl_3$ + CD_3OD): δ 17.7 (CH_3), 21.1 (CH_3), 30.7 (C-3′,5′), 33.7 (C-4′), 36.7 (C-1‴), 44.5 (C-2′,6′), 121.7 (C-2″,6″), 123.7 (C-4″), 125.7 (C-6⁗), 127.5 (C-4⁗), 129.2 (C-3″,5″), 131.0 (C-3⁗), 133.2 (C-2⁗), *N*-Ph [128.1 (*C*2,6), 131.1 (C-3,5), 131.3 (C-4), 133.3 (C-1)], 135.8 (C-5⁗), 136.7 (C-1⁗), 140.2 (C-1″), 152.6 (C-3), 157.2 (C═O), 159.7 (C-5), 168.1 (C-1‴); HR-EI-MS (*m/z*): 540.2325 $[M]^+$ calculated for $C_{30}H_{32}N_6O_2S$; 540.2307.

*4.7.8.4. 4-(5-(2-(2,6-Dimethylphenylamino)-2-oxoethylthio)-4-phenyl-4H-1,2,4-triazol-3-yl)-N-phenylpiperidine-1-carboxamide (**7l**).* White amorphous powder; Yield: 91%; M.P.: 190-148 ℃; IR (KBr) ν_{max}: 3359 (N—H), 3042 (Ar-H), 2969 (C—H), 1681, 1665 (C═O), 1617–1517 (Ar-C═C, C═N), 1261 (C—N); ^{1}H NMR (400 MHz, CD_3OD): δ 1.84 (4H, m, H-3′,5′), 2.14 (6H, s, CH_3), 2.76 (1H, m, H-4′), 2.80 (2H, m, H-2α′,6α′), 4.05 (2H, s, H-2‴), 4.14 (2H, br d, J = 13.2 Hz, H-2β′,6β′), 6.96 (1H, t, J = 8.5 Hz, H-4″), 7.05 (3H, m, H-3‴-5⁗), 7.22 (2H, t, J = 8.5 Hz, H-3″,5″), 7.29 (2H, d, J = 8.5 Hz, H-2″,6″), *N*-Ph [7.36 (2H, m, H-2,6), 7.61 (3H, m, H-3–5)]; ^{13}C NMR (100 MHz, $CDCl_3$ + CD_3OD): δ 18.4 (2 × CH_3), 30.6 (C-3′,5′), 33.6 (C-4′), 36.0 (C-1‴), 44.4 (C-2′,6′), 121.6 (C-2″,6″), 123.7 (C-4″), 128.1 (C-4⁗), 128.7 (C-3⁗,5⁗), 129.1 (C-3″,5″), *N*-Ph [128.0 (C-2,6), 131.1 (C-3,5), 131.5 (C-4), 133.1 (C-1)], 134.3 (C-1⁗), 136.1 (C-2⁗,6⁗), 140.1 (C-1″), 152.5 (C-3), 157.1 (C═O), 159.5 (C-5), 168.1 (C-1‴); HR-EI-MS (*m/z*): 540.2325 $[M]^+$ calculated for $C_{30}H_{32}N_6O_2S$; 540.2307.

*4.7.8.5. 4-(5-(2-(3,4-Dimethylphenylamino)-2-oxoethylthio)-4-phenyl-4H-1,2,4-triazol-3-yl)-N-phenylpiperidine-1-carboxamide (**7m**).* White amorphous powder; Yield: 90%; M.P.: 116-118 ℃; IR (KBr) ν_{max}: 3356 (N—H), 3049 (Ar-H), 2965 (C—H), 1686, 1669 (C═O), 1619–1519 (Ar-C═C, C═N), 1260 (C—N); ^{1}H NMR (400 MHz, CD_3OD): δ 1.83 (4H, m, H-3′,5′), 2.18 (3H, s, CH_3), 2.21 (3H, s, CH_3), 2.74 (1H, m, H-4′), 2.78 (2H, m, H-2α′,6α′), 3.94 (2H, s, H-2‴), 4.13 (2H, br d, J = 13.2 Hz, H-2β′,6β′), 6.97 (1H, t, J = 8.0 Hz, H-4″), 7.02 (1H, d, J = 8.0 Hz, H-6⁗), 7.22 (2H, t, J = 8.0 Hz, H-3″,5″), 7.27 (2H, m, H-2⁗,5⁗), 7.30 (2H, d, J = 8.0 Hz, H-2″,6″), *N*-Ph [7.33 (2H, m, H-2,6), 7.58 (3H, m, H-3–5)]; ^{13}C NMR (100 MHz, $CDCl_3$ + CD_3OD): δ 19.3 (CH_3), 20.0 (CH_3), 30.5 (C-3′,5′), 33.5 (C-4′), 37.1 (C-1‴), 44.3 (C-2′,6′), 121.5 (C-2″,6″), 118.1 (C-2⁗), 121.8 (C-6⁗), 123.6 (C-4″), 129.1 (C-3″,5″), 130.3 (C-5⁗), 133.0 (C-4⁗), *N*-Ph [127.8 (C-2,6), 130.9 (C-3,5), 131.4 (C-4), 133.4 (C-1)], 136.2 (C-3⁗), 137.6 (C-1⁗), 139.9 (C-1″), 152.5 (C-3), 156.9 (C═O), 159.3 (C-5), 167.0 (C-1‴); HR-EI-MS (*m/z*): 540.2325 $[M]^+$ calculated for $C_{30}H_{32}N_6O_2S$; 540.2307.

*4.7.8.6. 4-(5-(2-(Phenylamino)-2-oxoethylthio)-4-phenyl-4H-1,2,4-triazol-3-yl)-N-phenylpiperidine-1-carboxamide (**7n**).* White amorphous powder; Yield: 88%; M.P.: 145-155℃; IR (KBr) ν_{max}: 3359 (N—H), 3045 (Ar-H), 2966 (C—H), 1682, 1665 (C═O), 1617–1513 (Ar-C═C, C═N), 1261 (C—N); ^{1}H NMR (400 MHz, CD_3OD): δ 1.85 (4H, m, H-3′,5′), 2.17 (3H, s, CH_3), 2.27 (3H, s, CH_3), 2.80 (1H, m, H-4′), 2.84 (2H, m, H-2α′,6α′), 4.03 (2H, s, H-2‴), 4.15 (2H, br d, J = 13.2 Hz, H-2β′,6β′), 6.97 (1H, t, J = 8.5 Hz, H-4″), 7.03 (2H, s, H-2⁗,6⁗), 7.24 (2H, t, J = 8.5 Hz, H-3″,5″), 7.26 (1H, s, H-4⁗), 7.32 (2H, d, J = 8.0 Hz, H-2″,6″), *N*-Ph [7.46 (2H, m, H-2,6), 7.62 (3H, m, H-3–5)]; ^{13}C NMR (100 MHz, CD_3OD): δ 18.1 (CH_3), 21.0 (CH_3), 31.2 (C-3′,5′), 34.2 (C-4′), 37.1 (C-1‴), 44.9 (C-2′,6′), 122.2 (C-2″,6″), 124.1 (C-4″), 126.2 (C-2⁗), 127.8 (C-6⁗), 129.5 (C-3″,5″), 132.1 (C-4⁗), 133.5 (C-5⁗), *N*-Ph [128.8 (C-2,6), 131.4 (C-3,5), 131.8 (C-4), 134.0 (C-1)], 134.1 (C-3⁗), 137.2 (C-1⁗), 140.9 (C-1″), 152.7 (C-3), 157.8 (C═O), 160.4 (C-5), 168.8 (C-1‴); HR-EI-MS (*m/z*): 540.2325 $[M]^+$ calculated for $C_{30}H_{32}N_6O_2S$; 540.2307.

*4.7.8.7. 4-(5-(2-(3,6-Dimethylphenylamino)-2-oxoethylthio)-4-phenyl-4H-1,2,4-triazol-3-yl)-N-phenylpiperidine-1-carboxamide (**7o**).* White

amorphous powder; Yield: 91%; M.P.: 208-210℃; IR (KBr) ν_{max}: 3353 (N—H), 3041 (Ar-H), 2961 (C—H), 1680, 1666 (C═O), 1619–1519 (Ar-C═C, C═N), 1262 (C—N); ^{1}H NMR (400 MHz, CD_3OD): δ 1.83 (4H, m, H-3′,5′), 2.76 (1H, m, H-4′), 2.79 (2H, m, H-2α′,6α′), 3.96 (2H, s, H-2‴), 4.12 (2H, br d, J = 13.2 Hz, H-2β′,6β′), 6.98 (1H, t, J = 7.5 Hz, H-4″), 7.07 (1H, t, J = 7.5 Hz, H-4⁗), 7.22 (2H, t, J = 7.5 Hz, H-3″,5″), 7.29 (2H, t, J = 7.5 Hz, H-3⁗,5⁗), 7.33 (2H, d, J = 7.5 Hz, H-2″,6″), 7.36 (2H, d, J = 7.5 Hz, H-2⁗,6⁗), *N*-Ph [7.52 (2H, m, H-2,6), 7.58 (3H, m, H-3–5)]; ^{13}C NMR (100 MHz, $CDCl_3$ + CD_3OD): δ 30.5 (C-3′,5′), 33.4 (C-4′), 37.1 (C-2‴), 44.3 (C-2′,6′), 120.5 (C-2⁗,6⁗), 121.4 (C-2″,6″), 123.6 (C-4″), 125.0 (C-4⁗), 127.8 (C-3″,5″), 129.1 (C-3⁗,5⁗), *N*-Ph [129.4 (C-2,6), 130.9 (C-3,5), 131.4 (C-4), 132.9 (C-1)], 138.5 (C-1‴), 139.9 (C-1″), 152.5 (C-3), 156.9 (C═O), 159.3 (C-5), 167.2 (C-1‴); HR-EI-MS (*m/z*): 512.2014 $[M]^+$ calculated for $C_{28}H_{28}N_6O_2S$; 512.1994.

4.8. 15-LOX inhibition assay

The assay was performed according to the chemiluminescence method of Kondo and coworkers [25] with some minor modifications. A total volume of 100 μL of reaction mixture contained 60 μL of borate buffer (200 mM, pH 9.0), 10 μL of test compound or solvent, and 10 μL soybean 15-LOX enzyme. This mixture was incubated at 25 ℃ in dark for 5 min. Then 10 μL solution of luminol (3 nM) containing cytochrome-C (1 nM) was added to each well and luminescence was measured by BioTek HTX 96-well plate reader in luminescence mode. The reaction was initiated by the addition of 10 μL substrate solution (the substrate linoleic acid (155 μL) and Tween-20 (257 μL) were dissolved in 5 mL of deionized water followed by the addition of 0.6 mL 1 N NaOH and the mixture was emulsified). After dilution to 20 mL, this substrate solution was flushed with nitrogen gas to avoid the substrate from oxidation and used). Chemiluminescence of the reaction contents was measured for 100 to 300 s. All experiments were performed in triplicates. Quercetin was used as a positive control. The percentage of inhibition was calculated using the following formula:

Inhibition (%) = (Abs of control – Abs of test comp / Abs of control) × 100

The active compounds were serially diluted and their percentage inhibitions were determined. This data was used for the computation of IC_{50} using Ez–Fit Enzyme kinetics software (Perrella Scientific Inc. Amherst, USA).

4.9. Cell viability assay

Blood (3 mL) was collected in an EDTA tube from the healthy volunteer donors, which was diluted with PBS (phosphate buffer saline, 50 mM, pH 7.4) at 1:1 ratio. An equal volume of lymphocyte separation medium (density 1.077 g/mL, at 20 ℃, Cat. No. L0560 Lymphosep, Biowest, USA) was added in 15 mL Falcon tube. The diluted blood was then loaded onto the surface of the medium slowly to avoid the mixing of blood in the medium. The contents were centrifuged at 1200*g* for 20 min at 20℃ using a swing rotor. The ring of leukocytes was collected at the interface of lymphocyte separation medium and plasma by a Pasteur pipette. Collected cells were washed twice with 10 mL PBS 20 ℃ at 300*g*. The final pellet obtained was re-suspended in 0.5 mL PBS. RBCs and platelet pellets were discarded and Mononuclear Cells (MNCs) were washed with PBS and the total volume of MNCs was maintained to the required concentration. The dose-dependent response of the number of MNCs was constructed in the MTT assay. Volume (number of MNCs 6 × 10^5 per μL) of MNCs used per assay was linear in the tested range of 0–100 μL per well (data not shown).

MMT assay was carried out with some modifications as reviewed [21]. PBS (20 μL) was added per well followed by the addition of 10 μL test compounds (0.125 mM final concentration) or solvent and 60 μL MNCs in 96 well plate. The contents were incubated for two hours at 37 ℃. After a given time, 10 μL of 0.25 mg per mL MTT solution (3-(4,5-dimethylthiazol-2-yl)-2,5-diphenyltetrazolium bromide) was added per well. The plate was pre-read at 490 nm and incubated overnight for 18–20 h in an incubator at 37℃. After a given time, DMSO (100 μL) was added to dissolve the formazon crystals to make a total volume of 200 μL. Absorbance was measured after two hours. Experiments were carried out in triplicates along with the positive and negative controls. Cell viability was measured by the following equation.

Cell viability (%) = (Abs. of sample – Abs. of blank / Abs. of control – Abs. of blank) × 100.

Declaration of Competing Interest

The authors declare that they have no known competing financial interests or personal relationships that could have appeared to influence the work reported in this paper.

Acknowledgments

Thanks are due to the Higher Education Commission of Pakistan for funding the NRPU Project No. 4950 to M.A. and research assistantship to W.S. as well as the Alexander von Humboldt (AvH) Foundation, Germany for their financial support in the form of equipment grant.

Appendix A. Supplementary material

Supplementary data to this article can be found online at https://doi.org/10.1016/j.bioorg.2020.104525.

References

[1] S. Sinha, M. Doble, S.L. Manju, 5-Lipoxygenase as a drug target: a review on trends in inhibitors structural design, SAR and mechanism based approach, Bioorg. Med. Chem. 27 (2019) 3745–3759.
[2] J.R. Van, Y.S. Bakhlel, R.M. Botting, Cyclooxygenase 1 and 2, Ann. Rev. Pharmacol. Toxicol. 38 (1998) 97–120.
[3] H. Kuhn, S. Banthiya, K.V. Leyen, Mammalian lipoxygenases and their biological relevance, Biochim. Biophys. Acta 2015 (1851) 308–330.
[4] A. Liavonchanka, I. Feussner, Lipoxygenases: occurrence, functions and catalysis, J. Plant Physiol. 163 (2006) 348–357.
[5] A.D. Dobrian, M.A. Morris, D.A. Taylor-Fishwick, T.R. Holman, Y. Imai, R. G. Mirmira, J.L. Nadler, Role of the 12-lipoxygenase pathway in diabetes pathogenesis and complications, Pharmacol. Therapeut. 195 (2019) 100–110.
[6] H. Sadeghian, A. Jabbari, 15-Lipoxygenase inhibitors: a patent review, Exp. Opinion Therap. Pat. 26 (2016) 65–88.
[7] A. Orafaie, M.M. Matin, H. Sadeghian, The importance of 15-lipoxygenase inhibitors in cancer treatment, Cancer Metast. Rev. 37 (2018) 397–408.
[8] M.T. Maghraby, O.M. Abou-Ghadir, S.G. Abdel-Moty, A. Ali, O.A. Salem, Novel class of benzimidazole-thiazole hybrids: the privileged scaffolds of potent anti-inflammatory activity with dual inhibition of cyclooxygenase and 15-lipoxygenase enzymes, Bioorg. Med. Chem. 28 (2020), 115403.
[9] P. Lu, M.L. Schraq, D.E. Slaughter, C.E. Raab, Mechanism based inhibition of human liver microsomal cuytochrome P450 1A2 by Zileuton, a 5-lipoxygenase inhibitor, Drug Metabol. Disposit. 31 (2003) 1352–1360.
[10] E. Skrzypczak-Jankun, J. Chorostowska-Wynimko, S.H. Selman, J. Jankun, Lipoxygenases – a challenging problem in enzyme inhibition and drug development, Curr. Enz. Inhib. 3 (2007) 119–132.
[11] S. Maddila, R. Pagadala, S.B. Jonnalagadda, 1,2,4-triazoles: a review of synthetic approaches and the biological activity, Lett. Org. Chem. 10 (2013) 693–714.
[12] E. Gultekin, Y. Kolcuoglu, A. Akdemir, Y. Sirin, H. Bektas, O. Bekircan, A study on synthesis, biological activities and molecular modelling of some novel trisubstituted 1,2,4-triazole derivatives, Chem. Select 3 (2018) 8813–8818.
[13] C.-H. Zhou, Y. Wang, Recent researches in triazole compounds as medicinal drugs, Cur. Med. Chem. 19 (2012) 239–280.
[14] N.S. Mahajan, A.M. Manikrao, P.N. Shinde, R.D. Jawarkar, P.N. Khatale, S.C. Dhawale, A review: Biological importance of mercapto substituted 1,2,4-triazole derivatives, R. Kharb, P.C. Sharma, M.S. Yar, Pharmacological significance of triazole scaffold, J. Enz. Inhib. Med. Chem., 26 (2011) 1-21.
[15] M.-X. Song, X.-Q. Deng, Recent developments on triazole nucleus in anticonvulsant compounds: a review, J. Enzyme Inhibition Med. Chem. 33 (2018) 453–478.
[16] S. Ram, G. Celik, P. Khloya, D. Vullo, C.T. Supuran, P.K. Sharma, Benzenesulfonamide bearing 1,2,4-triazole scaffolds as potent inhibitors of tumor associated carbonic anhydrase isoforms hCA IX and hCA XII, Bioorg. Med. Chem. 22 (2014) 1873–1882.

[17] T. Sato, N. Ashizawa, T. Iwanaga, H. Nakamura, K. Matsumoto, T. Inoue, O. Nagata, Design, synthesis, pharmacological and pharmacokinetic evaluation of 3-phenyl-5-pyridyl-1,2,4-triazole derivatives as xanthine oxidoreductase inhibitors, Bioorg. Med. Chem. Lett. 19 (2009) 184–187.
[18] J.P. Marino, P.W. Fisher, G.A. Hofmann, R.B. Kirkpatrick, C.A. Janson, R. K. Johnson, C.M. Mattern, T.D. Meek, M.D. Ryan, C. Schulz, W.W. Smith, D.G. Tew, T.A. Tomazek, D.F. Veber, W.C. Xiong, Y. Yamamoto, K. Yamashita, G. Yang, S. K. Thompson, Highly potent inhibitors of methionine aminopeptidase-2 based on a 1,2,4-triazole pharmacophore, J. Med. Chem. 50 (2007) 3777–3785.
[19] S.A. Shahzad, M. Yar, Z.A. Khan, L. Shahzadi, S. Naqvi, A. Mahmood, S. Ullah, A. J. Shaikh, T. Sherazi, A.T. Bale, J. Kukułowicz, M. Bajda, Identification of 1,2,4-triazoles as new thymidine phosphorylase inhibitors: future anti-tumor drugs, Bioorg. Chem. 85 (2019) 209–220.
[20] H. Cai, X. Huang, S. Xu, H. Shen, P. Zhang, Y. Huang, J. Jiang, Y. Sun, B. Jiang, X. Wu, H. Yao, J. Xu, Discovery of novel hybrids of diaryl-1,2,4-triazoles and caffeic acid as dual inhibitors of cyclooxygenase-2 and 5-lipoxygenase for cancer therapy, Eur. J. Med. Chem. 108 (2016) 89–103.
[21] J.C. Stockert, R.W. Horobin, L.L. Colombo, A. Blázquez-Castro, Tetrazolium salts and formazan products in cell biology: viability assessment, fluorescence imaging, and labeling perspectives, Acta Histochem. 120 (2018) 159–167.
[22] D.F. Veber, S.R. Johnson, H.Y. Cheng, B.R. Smith, K.W. Ward, K.D. Kopple, Molecular properties that influence the oral bioavailability of drug candidates, J. Med. Chem. 45 (2002) 2615–2623.
[23] C.A. Lipinski, F. Lombardo, B.W. Domini, P.J. Feeney, Experimental and computational approaches to estimate solubility and permeability in drug discovery and development settings, Adv. Drug Deliver. Rev. 23 (1997) 4–25.
[24] S.M. Seyedi, H. Eshghi, Z. Jafari, N. Attaran, H. Sadeghian, M.R. Saberi, M. M. Riazi, Design, synthesis and SAR studies of 4-allyoxyaniline amides as potent 15-lipoxygensae inhibitors, Bioorg. Med. Chem. 17 (2009) 1614–1622.
[25] Y. Kondo, Y. Kawai, T. Miyazawa, H. Matsui, J. Mizutani, An assay for lipoxygenase activity by chemiluminescence, Biosci. Biotech. Biochem. 58 (1994) 421–422.